

Contents lists available at [ScienceDirect](http://ScienceDirect)

# Journal of Rock Mechanics and Geotechnical Engineering

journal homepage: [www.rockgeotech.org](http://www.rockgeotech.org)

## Full Length Article

# The Hoek–Brown failure criterion and GSI – 2018 edition

E. Hoek<sup>a,\*</sup>, E.T. Brown<sup>b</sup><sup>a</sup> North Vancouver, British Columbia, V7R 4H7, Canada<sup>b</sup> Brisbane, Queensland 4169, Australia

## ARTICLE INFO

### Article history:

Received 22 July 2018

Received in revised form

2 August 2018

Accepted 3 August 2018

Available online xxx

### Keywords:

Hoek–Brown criterion

Geological strength index (GSI)

Rock mass strength

Uniaxial compressive strength (UCS)

Tension cut-off

Rock mass deformation modulus

## ABSTRACT

The Hoek–Brown criterion was introduced in 1980 to provide input for the design of underground excavations in rock. The criterion now incorporates both intact rock and discontinuities, such as joints, characterized by the geological strength index (GSI), into a system designed to estimate the mechanical behaviour of typical rock masses encountered in tunnels, slopes and foundations. The strength and deformation properties of intact rock, derived from laboratory tests, are reduced based on the properties of discontinuities in the rock mass. The nonlinear Hoek–Brown criterion for rock masses is widely accepted and has been applied in many projects around the world. While, in general, it has been found to provide satisfactory estimates, there are several questions on the limits of its applicability and on the inaccuracies related to the quality of the input data. This paper introduces relatively few fundamental changes, but it does discuss many of the issues of utilization and presents case histories to demonstrate practical applications of the criterion and the GSI system.

© 2018 Institute of Rock and Soil Mechanics, Chinese Academy of Sciences. Production and hosting by Elsevier B.V. This is an open access article under the CC BY-NC-ND license (<http://creativecommons.org/licenses/by-nc-nd/4.0/>).

## 1. Introduction

The Hoek–Brown criterion was derived from the results of research into the brittle failure of intact rock by [Hoek \(1965\)](#) and on model studies of jointed rock mass behaviour by [Brown \(1970\)](#).

The brittle fracture theory published by [Griffith \(1924\)](#), modified by [McClintock and Walsh \(1962\)](#) to account for friction on sliding surfaces, formed the basis for the nonlinear failure criterion for intact rock published by [Hoek and Brown \(1980a, b\)](#). This 2018 edition of the criterion incorporates all the modifications that have been implemented in the past 38 years, based on experiences gained in applying this criterion to practical problems.

The geological strength index (GSI) is a system of rock mass characterization that was developed, by [Hoek \(1994\)](#) and [Hoek et al. \(1995\)](#), to link the failure criterion to engineering geology observations in the field. The most complete description of the current use of the GSI and the Hoek–Brown criterion is given in a chapter entitled “Rock mass properties” in an eBook by Hoek, called *Practical Rock Engineering*, which can be downloaded from <http://www.rocsience.com>.

\* Corresponding author.

E-mail addresses: [ehoek@mailas.com](mailto:ehoek@mailas.com) (E. Hoek), [et\\_brown@bigpond.com](mailto:et_brown@bigpond.com) (E.T. Brown).

Peer review under responsibility of Institute of Rock and Soil Mechanics, Chinese Academy of Sciences.

<https://doi.org/10.1016/j.jrmge.2018.08.001>

1674-7755 © 2018 Institute of Rock and Soil Mechanics, Chinese Academy of Sciences. Production and hosting by Elsevier B.V. This is an open access article under the CC BY-NC-ND license (<http://creativecommons.org/licenses/by-nc-nd/4.0/>).

The Hoek–Brown failure criterion and the associated GSI have gained wide acceptance as tools for estimating the strength and deformation characteristics of heavily jointed rock masses. Because of the lack of suitable alternatives, the criterion was adopted by the rock mechanics community and its use quickly spread beyond the original assumptions based on interlocking joint-defined blocks in hard rocks. Consequently, it became necessary to re-examine these assumptions and to introduce new elements from time to time to account for the wide range of practical problems to which the criterion was being applied.

One of the early difficulties arose because many geotechnical problems, particularly slope stability issues, are more conveniently dealt with in terms of shear and normal stresses rather than the principal stresses used in the definition of the original Hoek–Brown criterion. At that time, geotechnical software did not allow the incorporation of the constitutive relationships, including flow rules that describe the behaviour of the rock after reaching the peak strength predicted by the Hoek–Brown criterion. Hence, it was necessary to find equivalent Mohr–Coulomb parameters for use with existing software. In 2018, most geotechnical software for stress and slope stability analysis allows the Hoek–Brown criterion to be used directly. Consequently, in this context, only the Hoek–Brown criterion is discussed in detail.

For readers who require equivalent Mohr–Coulomb friction angles and cohesive strengths, a detailed discussion on how these can be obtained is given in [Hoek et al. \(2002\)](#). It is recommended

that these friction angles and cohesive strengths, derived from the Hoek–Brown criterion, should not be used without a tension cut-off.

The GSI was extended to cover folded and tectonically sheared rock masses in a series of papers by Hoek et al. (1998, 2005), Hoek and Marinos (2000), Marinos and Hoek (2000, 2001), Marinos (2017), Marinos et al. (2005), and Marinos and Carter (2018). The GSI is discussed in detail in Sections 6 and 11.

For clarity, the equations provided and discussed here are expressed in total stress terms. However, as discussed by Hoek and Brown (1997), the solution to some rock engineering problems requires an effective stress approach. In this case, effective stress equivalents of the equations given here may be used.

## 2. The origin of the Hoek–Brown criterion

There is abundant evidence to show that the failure in brittle materials such as rock, concrete, ceramic and glass originates from micro-cracks or flaws in the intact material. In rock, these flaws are typically grain boundaries or inter-granular cracks and tensile cracks that propagate from their tips when frictional sliding occurs along the flaw.

Griffith (1921) proposed that tensile failure in brittle materials such as glass initiates at the tips of defects which he represented by flat elliptical cracks. His original work dealt with fracture in material subjected to tensile stress, but later he extended this concept to include biaxial compression loading (Griffith, 1924), thereby obtaining a nonlinear compressive failure envelope for brittle materials.

Murrell (1958) proposed the application of the Griffith theory to rock. This suggestion was immediately implemented by researchers such as McClintock and Walsh (1962), Brace (1964), Hoek (1964), Cook (1965) and many others. The early findings of this research were summarized by Jaeger and Cook (1969). More recent research has been summarized by Andriev (1995).

Based on this research on the nonlinear Griffith failure criterion, Hoek and Brown (1980a, b) proposed the following empirical equation to fit the results of a wide range of triaxial tests on intact rock samples:

$$\sigma_1 = \sigma_3 + \sigma_{ci} \sqrt{m_i \frac{\sigma_3}{\sigma_{ci}} + 1} \quad (1)$$

where  $\sigma_1$  and  $\sigma_3$  are the major and minor principal stresses, respectively;  $\sigma_{ci}$  is the unconfined compressive strength; and  $m_i$  is a material constant for the intact rock.

Zuo et al. (2008, 2015) showed that a very similar equation could be derived from an analysis of failure propagation from a penny-shaped crack in a triaxial stress field. Their equation can be written:

$$\sigma_1 = \sigma_3 + \sigma_{ci} \sqrt{\left(\frac{\mu}{\kappa} \frac{\sigma_{ci}}{|\sigma_t|}\right) \frac{\sigma_3}{\sigma_{ci}} + 1} \quad (2)$$

where  $\mu = \tan \phi$  ( $\phi$  is the crack surface friction angle);  $\kappa$  is a coefficient used for mixed mode fracture which can be derived from various approximations, such as  $\kappa = \sqrt{3/2}$  for a maximum stress criterion, with  $\kappa = 1$  for a maximum energy release criterion; and  $|\sigma_t|$  is the absolute value of the uniaxial tensile strength.

Substitution of  $m_i = \mu \sigma_{ci} / (\kappa |\sigma_t|)$  in Eq. (2) results in the Hoek–Brown Eq. (1) for intact rock. Hence, the constant  $m_i$  has a physical meaning. As will be shown later in this paper, the relationship between  $m_i$  and  $\sigma_{ci}/|\sigma_t|$  is important in the application of the Hoek–Brown criterion to rock and rock mass failure.

## 3. Generalized Hoek–Brown criterion

The generalized Hoek–Brown criterion for the estimation of rock mass strength, introduced by Hoek (1994) and Hoek et al. (1995), is expressed as

$$\sigma_1 = \sigma_3 + \sigma_{ci} \left( m_b \frac{\sigma_3}{\sigma_{ci}} + s \right)^a \quad (3)$$

where  $m_b$ ,  $s$ , and  $a$  are the rock mass material constants, given by

$$m_b = m_i \exp[(GSI - 100)/(28 - 14D)] \quad (4)$$

$$s = \exp[(GSI - 100)/(9 - 3D)] \quad (5)$$

$$a = 1/2 + 1/6 \left( e^{-GSI/15} - e^{-20/3} \right) \quad (6)$$

where, for intact rock, the material constants are denoted by  $m_i$ ,  $s = 1$  and  $a = 0.5$ ;  $D$  is a factor which depends upon the degree of disturbance to which the rock mass has been subjected to blast damage and stress relaxation. Guidelines for the selection of  $D$  are discussed in Section 8.

Eqs. (4)–(6) were developed to deal with rock masses, such as that illustrated in Fig. 1, comprised of interlocking angular blocks in which the failure process is dominated by block sliding and rotation without a great deal of intact rock failure, under low to moderate confining stresses.

In dealing with the application of Eqs. (4)–(6) to rock masses which fall outside the range of conditions as described above, several authors have proposed modifications to the values of the constants or even the form of these equations. This is a completely



Fig. 1. Interlocking blocks of very strong Panguna andesite and granodiorite in the Bougainville open pit mine in Papua New Guinea for which the original Hoek–Brown criterion for rock mass strength estimation was developed (Hoek and Brown, 1980a, b).

understandable and acceptable approach. However, readers intending to apply these modifications should ensure that they have done sufficient reading and research to enable them to define the range of applicability of these modifications and whether they apply to the problem under consideration. In other words, do not apply equations, other than Eqs. (4)–(6), simply because they appear to be new or interesting.

Originally, the GSI term in these equations was estimated directly from Bieniawski’s rock mass rating (RMR) classification (Brown and Hoek, 1988). The GSI was introduced by Hoek (1994) as a direct replacement for RMR.

**4. Strength of intact rock**

In Eq. (3), the unconfined compressive strength,  $\sigma_{ci}$ , is the dominant parameter which sets the scale of the rock mass strength failure curve on a  $\sigma_1$  vs  $\sigma_3$  plot. The constants  $m_b$ ,  $s$ , and  $a$  define the shape of the curvilinear failure plot. At this point, it is important to explain the difference between the unconfined compressive strength,  $\sigma_{ci}$ , and the uniaxial compressive strength (UCS) of intact rock. The UCS is generally determined by testing several specimens without applying a confining stress. Fig. 2 shows the distribution curves obtained from high quality laboratory UCS tests on a range of rock types encountered on a typical construction project.

In developing the Hoek–Brown criterion, it was recognized that including a collection of UCS test results in a series of triaxial test data would result in a significant bias in the curve fitting process required to determine the constants of the equation. Consequently, it was decided to use only the average value for a UCS data set to represent the value of the principal stress at zero confining stress. The triaxial data set, including this average value, was then used in a regression analysis to determine the unconfined compressive strength,  $\sigma_{ci}$ , and the constant,  $m_i$ .

The Hoek–Brown criterion was developed to deal with shear failure in rock. Fig. 3 plotting the results of triaxial compression tests on Indiana limestone by Schwartz (1964) shows that the range of applicability of the criterion is determined by the transition from shear to ductile failure at approximately  $\sigma_1 = 4.0\sigma_3$ . Mogi (1966) investigated the transition from shear to ductile failure in a wide range of rock types and found that the average transition is defined by  $\sigma_1 = 3.4\sigma_3$ . This is a useful guide for the maximum confining pressure for triaxial testing of intact

rock specimens. In some laboratories, triaxial tests are carried out by applying a constant confining stress and increasing the axial load until the onset of shear failure is detected in the stress–strain plot. The confining stress is then increased, and the axial load is again increased until the onset of the next failure is detected. This stage testing process is repeated several times to arrive at a complete failure plot from a single specimen. Since the specimen has been damaged in the first loading cycle and all subsequent test stages involve the damaged rock, this method does not produce an acceptable peak strength plot for intact rock. Therefore, it is recommended that this type of triaxial test should not be used for determining the Hoek–Brown parameters  $\sigma_{ci}$  and  $m_i$ .

Tensile failure ( $\sigma_3 < 0$ ) is not dealt with by the Hoek–Brown criterion. However, tensile failure is an important factor in some rock engineering problems. In the context of this discussion, the most effective solution to this problem is the Griffith theory which, as proposed by Fairhurst (1964), can be generalized in terms of the ratio of compressive to tensile strength,  $\sigma_{ci}/|\sigma_t|$ , as follows:

- (1) If  $w(w - 2)\sigma_3 + \sigma_1 \leq 0$ , failure occurs when  $\sigma_3 = \sigma_t$
- (2) If  $w(w - 2)\sigma_3 + \sigma_1 > 0$ , failure occurs when

$$\sigma_1 = \frac{(2\sigma_3 - A\sigma_t) + \sqrt{(A\sigma_t - 2\sigma_3)^2 - 4(\sigma_3^2 + A\sigma_t\sigma_3 + 2AB\sigma_t^2)}}{2} \tag{7}$$

where

$$A = 2(w - 1)^2, B = \left(\frac{w - 1}{2}\right)^2 - 1, w = \sqrt{\frac{\sigma_{ci}}{|\sigma_t|} + 1}$$

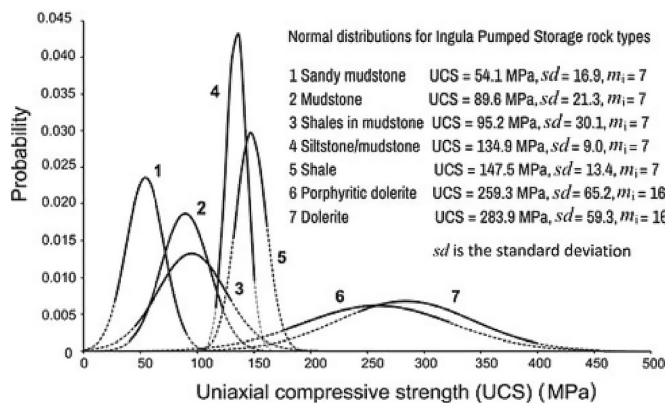


Fig. 2. Normal distributions and UCS values determined from tests on cores from seven rock types recovered during the site investigation and design phase for the Ingula Pumped Storage Project in South Africa (Keyter et al., 2008).

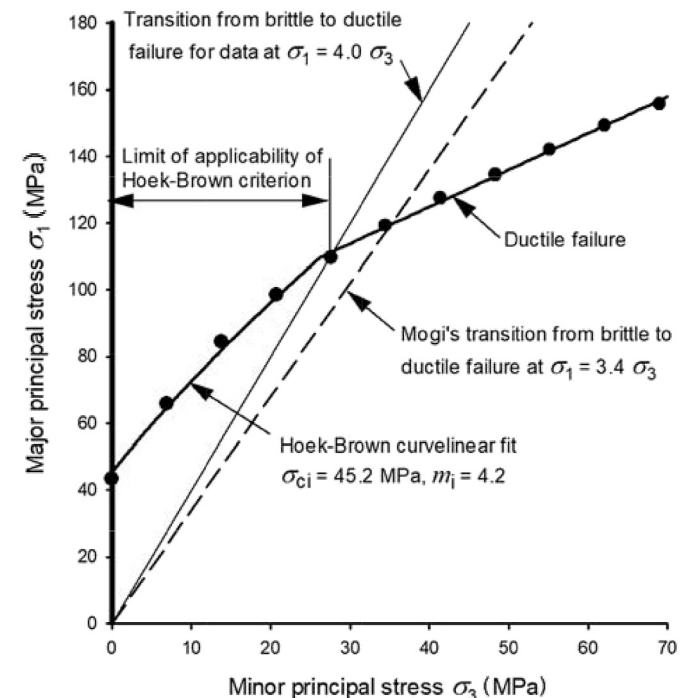


Fig. 3. Limit of applicability of the Hoek–Brown criterion and for the maximum confining pressure for triaxial tests on Indiana limestone.

The combination of two failure criteria on one plot can result in significant complications in programming for numerical analyses. Therefore, it is preferable to simplify the resulting combination as far as possible. Hoek and Martin (2014) proposed that, for practical rock engineering purposes, a Hoek–Brown failure envelope with a tensile cut-off, based on the generalized Griffith failure criterion theory proposed by Fairhurst (1964), can provide an effective solution. This is illustrated in the plot presented in Fig. 4.

The tests conducted by Ramsey and Chester (2004) and Bobich (2005) are among the very few reliable triaxial data sets which include direct tensile tests. Some suggestions on testing procedures required to provide reliable data are given in the Appendix. As an interim measure, the following approximate relationship between the compressive to tensile strength ratio,  $\sigma_{ci}/\sigma_t$ , and the Hoek–Brown parameter  $m_i$  is proposed:

$$\sigma_{ci}/\sigma_t = 0.81m_i + 7 \quad (8)$$

Eq. (8) is based on triaxial test data and curve fitting estimates, as listed in Table 1 and plotted in Fig. 5.

An example of plotting the Hoek–Brown failure curve with a tension cut-off is presented in Fig. 6. The data for this plot were obtained from triaxial tests on specimens of Granite Aplite, a uniformly fine grained intrusive igneous rock from South Africa. These tests were carried out by Dr. W. Brace at Massachusetts Institute of Technology in the USA and Dr. E. Hoek at the Council for Scientific and Industrial Research in South Africa. The average unconfined compressive strength of 588 MPa was used, with the triaxial test results, to fit the peak strength curve. The tension cut-off was calculated using Eq. (8).

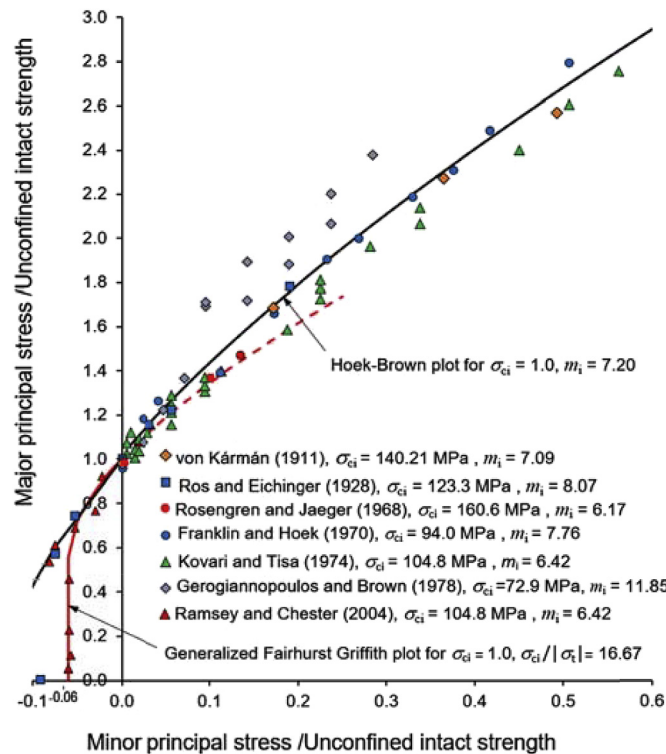


Fig. 4. Dimensionless plot of triaxial test data for Carrara marble showing the use of the generalized Griffith theory for tensile failure and the Hoek–Brown criterion for shear failure. (Von Kármán, 1911, Ros et al., 1928, Rosengren and Jaeger, 1968, Franklin and Hoek, 1970, Kovari and Tisa, 1974, Gerogiannopoulos and Brown, 1978, Ramamurthy, 1993, Kalamaris and Bieniawski, 1995, Sheorey, 1997, Aydan and Dalgiç, 1998).

Table 1  
Analysis of data containing tensile values.

$\sigma_{ci}$ (MPa)	$m_i$	$\sigma_{ci}/ \sigma_t $	Data set
224	32.4	32	Granite (Lau and Gorski, 1992)
600.4	18.8	22.2	Granite Aplite (Hoek, 1965)
95.5	9.65	14.9	Berea sandstone (Bobich, 2005)
125.5	10.6	14.4	Webtuck dolomite (Brace, 1964)
516.5	8.45	13.9	Blair dolomite (Brace, 1964)
128.5	8.25	16.6	Marble (Ramsey and Chester, 2004)
228	14.1	18.6	Quartzite (Hoek, 1965)
1	5	10	Estimated by matching Hoek–
1	7.2	12	Brown and Fairhurst generalized
1	10	14	Griffith curves as illustrated in Fig. 4.
1	15	20	
1	20	24	
1	30	32	

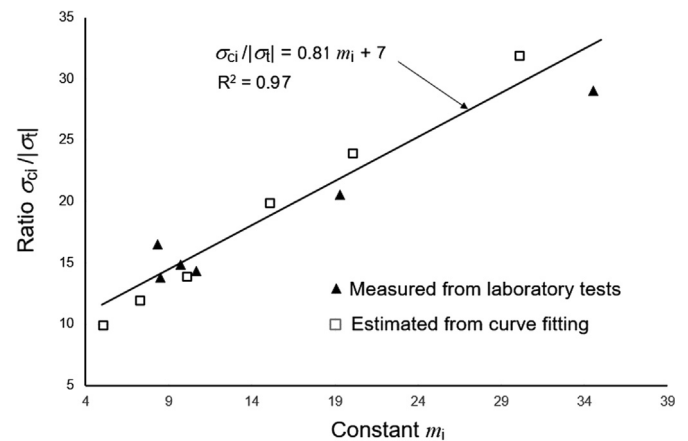


Fig. 5. Relationship between  $\sigma_{ci}/|\sigma_t|$  and  $m_i$ .

It will be noted that, for intact rock, only two variables are needed to define the Hoek–Brown failure envelope with a tension cut-off. These are the unconfined compressive strength of the intact rock,  $\sigma_{ci}$ , and the material parameter,  $m_i$ . For hard intact rock, the parameter  $s$  is always equal to 1 and the constant  $a \approx 0.5$ .

Note that the Brazilian test, in which the tensile failure is induced as a centre of a diametrically loaded disc specimen, is not an acceptable direct tensile test for inclusion in the analysis as described above. Due to the complex stress distribution and the influence of the stress concentrations at the loading points, the calculation of the tensile strength requires significant correction (Perras and Diederichs, 2014). At best, the Brazilian test can be regarded as an index test which must be calibrated against direct tensile tests for each rock type.

### 5. Limits of applicability of the Hoek–Brown criterion

Fig. 3 shows that the Hoek–Brown criterion is only applicable for confining stresses within the range defined by  $\sigma_3 = 0$  and the transition from shear to ductile failure.

A case in which the Hoek–Brown criterion does not apply may arise when massive rock is in a state of relatively high confinement. Kaiser et al. (2010) discuss this case in the context of highly stressed pillars in hard, brittle rock at depth. In this case, it was found that the amount of rock mass strength degradation given by Eqs. (4) and (5) for  $m_b$  and  $s$  was reduced by replacing the constants 28, in Eq (4), and 9, in Eq (5) with higher values that Kaiser et al. (2010) related to the GSI and confining pressure. Importantly, in this case, higher

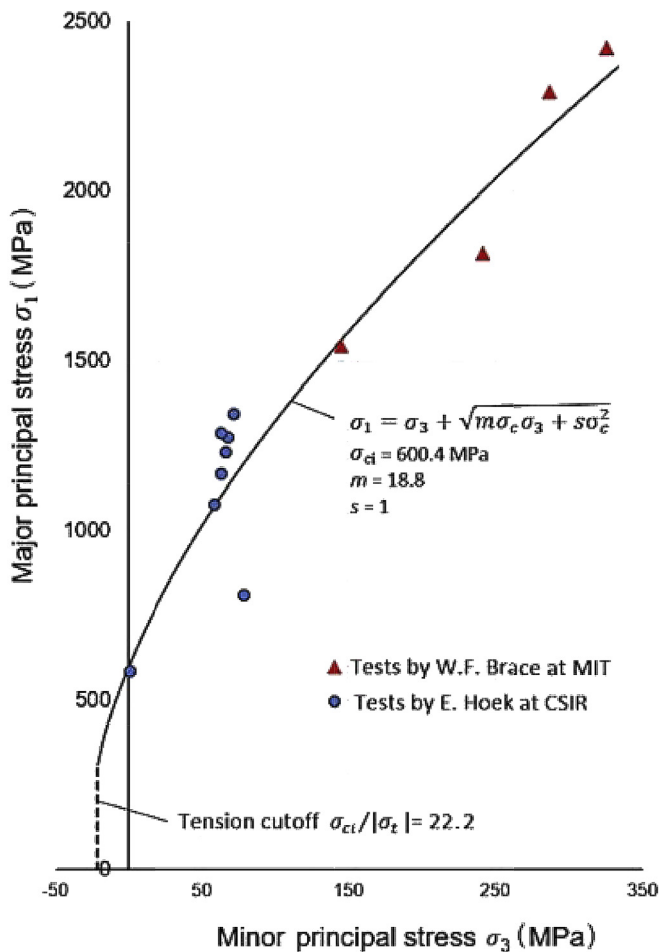


Fig. 6. Hoek–Brown failure plot for triaxial tests on Granite Aplite carried out by Hoek (1965) and Brace (1964).

confinement produced rock mass strengths that were greater than those given by the conventional application of Eqs. (3)–(6).

A more general case in which Eqs. (3)–(6) may not apply is in massive to moderately jointed hard rock having high values of GSI. For example, for  $GSI \geq 65$ , Bewick et al. (2019) show how carefully distinguishing the failure modes of heterogeneous hard rock specimens in laboratory uniaxial and triaxial compression strength tests can allow the conventional Hoek–Brown criterion and GSI approach to be used for strength estimation. The parameters should be adjusted to provide good fits to test data for massive to moderately jointed rock.

## 6. The geological strength index (GSI)

Hoek (1994) and Hoek et al. (1995) introduced the GSI as a tool for collecting field information for incorporation in Eqs. (4)–(6). This is used to estimate the constants  $m_i$ ,  $s$  and  $a$  in the Hoek–Brown criterion defined by Eq. (3). The GSI classification was set up to address the two principal factors considered to have important influences on the mechanical properties of a rock mass, i.e. the structure (or blockiness) and the condition of the joints. The latest major revision of the GSI and its use in Eqs. (4)–(6) was made by Hoek et al. (2002). The basic version of the GSI chart, for use with jointed rocks, is reproduced in Fig. 7, from Hoek and Marinos (2000).

The Hoek–Brown failure criterion was originally developed based on the assumption that intact rock is free from defects other than microcracks and flaws. The GSI system was developed to deal with rock masses comprised of interlocking angular blocks in which the failure process is dominated by block sliding and rotation without a great deal of intact rock failure.

Figs. 8–12 show the typical applications of the GSI chart to exposed faces in a range of rock formations. The original purpose of the GSI chart was to provide a guide for the initial estimation of rock mass properties. It was always assumed that the user would improve the initial estimates with more detailed site investigations, numerical analyses, and back analyses of the tunnel or slope performance to validate or modify these estimates.

In dealing with the tectonically disturbed rock masses, as illustrated in Figs. 10 and 11, the original GSI chart is adequate for estimates during the site investigation stage. However, during the later design stages, it becomes more difficult to apply this chart effectively unless observations and measurements of the rock mass behaviours in response to excavation are available to provide a basis for calibration.

To simplify this problem, Marinos and Hoek (2001) published a GSI chart for heterogeneous and tectonically deformed sedimentary rocks. An extended version of this chart was published by Marinos (2017) and Marinos and Carter (2018). Additional charts for ophiolites (Marinos et al., 2005) and tectonically undisturbed molassic rocks (Hoek et al., 2005) were also developed to cover tunnelling projects in northern Greece.

## 7. Estimating rock mass deformation modulus

In addition to the estimate of the strength of intact rock and rock masses, the analysis of the behaviour of a slope, foundation or tunnel also requires an estimate of the deformation modulus of the rock mass in which these structures are excavated. This is a significant challenge and numerous authors have presented various suggestions on how these estimates can be made.

Hoek and Diederichs (2006), using a database of rock mass deformation modulus measurements from projects in China (including Taiwan), proposed the following equation for estimating rock mass modulus (Fig. 13):

$$E_{rm} = E_i \left\{ 0.02 + \frac{1 - D/2}{1 + \exp[(60 + 15D - GSI)/11]} \right\} \quad (9)$$

where  $E_i$  is the intact rock deformation modulus (MPa).

Hoek and Diederichs (2006) recommended that, when the laboratory measured values for  $E_i$  are not available, the rock mass reduction values (MR) proposed by Deere (1968) can be used for estimating the intact rock modulus. When no information on the intact rock deformation modulus is available, the following alternative equation for estimating the rock mass modulus  $E_{rm}$  (MPa) was proposed by Hoek and Diederichs (2006):

$$E_{rm} = 10^5 \frac{1 - D/2}{1 + \exp[(75 + 25D - GSI)/11]} \quad (10)$$

Fig. 14 gives a comparison between the deformation modulus estimated from Eq. (10) and a number of field measurements and predictions by Bieniawski (1978), Serafim and Pereira (1983), Stephens and Banks (1989), Read et al. (1999), and Barton (2002). The general agreement between these results suggests that all these predictions, including those of Hoek and Diederichs (2006), can be used with confidence for estimating field values.

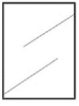
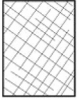




<p>GEOLOGICAL STRENGTH INDEX FOR JOINTED ROCKS (Hoek and Marinos, 2000)</p> <p>From the lithology, structure and surface conditions of the discontinuities, estimate the average value of GSI. Do not try to be too precise. Quoting a range from 33 to 37 is more realistic than stating that GSI = 35. Note that the table does not apply to structurally controlled failures. Where weak planar structural planes are present in an unfavourable orientation with respect to the excavation face, these will dominate the rock mass behaviour. The shear strength of surfaces in rocks that are prone to deterioration as a result of changes in moisture content will be reduced if water is present. When working with rocks in the fair to very poor categories, a shift to the right may be made for wet conditions. Water pressure is dealt with by effective stress analysis.</p>		SURFACE CONDITIONS				
STRUCTURE		DECREASING SURFACE QUALITY →				
		VERY GOOD Very rough, fresh unweathered surfaces	GOOD Rough, slightly weathered, iron stained surfaces	FAIR Smooth, moderately weathered and altered surfaces	POOR Slackensided, highly weathered surfaces with compact coatings or fillings or angular fragments	VERY POOR Slackensided, highly weathered surfaces with soft clay coatings or fillings
	INTACT OR MASSIVE - intact rock specimens or massive in situ rock with few widely spaced discontinuities	90			N/A	N/A
	BLOCKY - well interlocked undisturbed rock mass consisting of cubical blocks formed by three intersecting discontinuity sets	80	70			
	VERY BLOCKY- interlocked, partially disturbed mass with multi-faceted angular blocks formed by 4 or more joint sets		60	50		
	BLOCKY/DISTURBED/SEAMY - folded with angular blocks formed by many intersecting discontinuity sets. Persistence of bedding planes or schistosity			40	30	
	DISINTEGRATED - poorly interlocked, heavily broken rock mass with mixture of angular and rounded rock pieces				20	
	LAMINATED/SHEARED - Lack of blockiness due to close spacing of weak schistosity or shear planes	N/A	N/A			10

Fig. 7. Basic GSI chart (Hoek and Marinos, 2000).

Cai et al. (2004) carried out a detailed review of the application of the GSI system for the estimation of rock mass strength and deformation properties in two underground powerhouse projects in Japan. In their conclusion they state:

*“The GSI system was applied to characterize the jointed rock masses at Kannagawa and Kazunogawa underground powerhouses in Japan. Based on the estimated GSI values and intact rock strength properties, equivalent Mohr–Coulomb strength parameters and elastic modulus of the jointed rock mass were calculated and compared to in situ test results. The Point Estimate Method was applied to approximate variance of the mechanical properties of the jointed rock masses. It is found that both the means and variances of  $c$ ,  $\phi$  and  $E$  predicted from the quantified GSI approach are generally in good agreement with field data. Hence, the quantitative approach added to the GSI system provides a means*

*for consistent rock mass characterization and thus improves the utility of the GSI system.”*

**8. Disturbance factor  $D$**

When tunnels, slopes or foundations are excavated in rock masses, removal of the rock results in stress relief which allows the surrounding rock mass to relax and dilate. The aim of any good design is to control this dilation, and the consequent displacements, in order to minimize rock failure. This can be achieved by a careful selection of excavation shape, method of excavation and, if necessary, the installation of reinforcement and support. In many cases, drainage of the rock mass is also an important factor in maintaining the stability of the excavation.

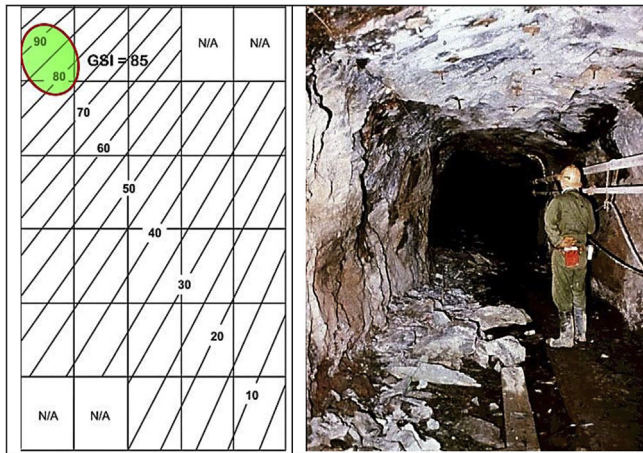


Fig. 8. Spalling in the sidewalls of a mine tunnel in intact hard rock subjected to anisotropic horizontal stresses. GSI is not applicable in the analysis of these stress-induced spalls but it can be used for other applications.

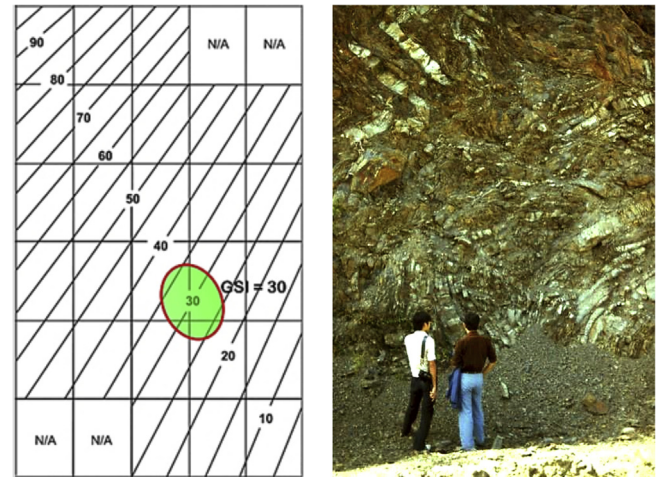


Fig. 11. Complex folding in a bedded sedimentary deposit. GSI is applicable with care since averaging of the intact properties is required to calculate rock mass properties.

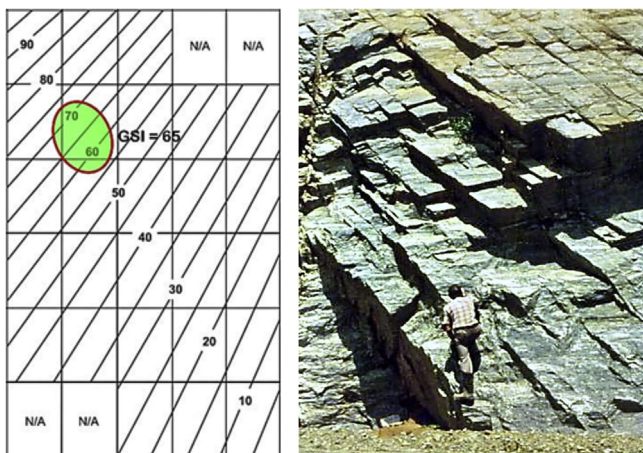


Fig. 9. Orthogonal jointing in granitic rock on a dam site. GSI is not applicable on this scale since the stability of the exposed face is controlled by the geometry of intersecting joints. It can be applied to larger scale excavations.

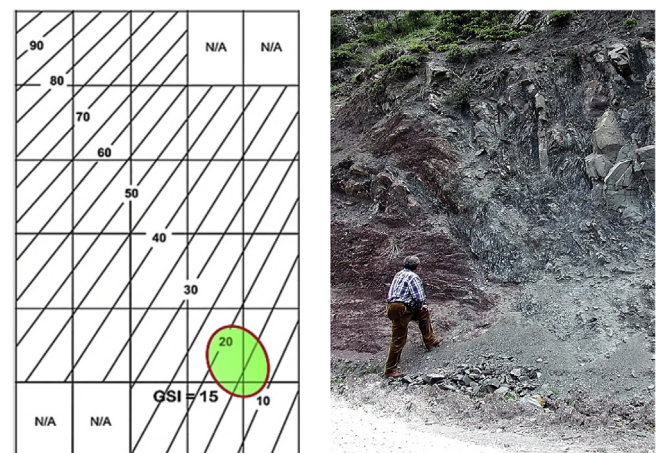


Fig. 12. Tectonically deformed sediments with almost complete loss of structural patterns. Care is required in using GSI in this type of rock mass. Use the GSI charts by Marinos et al. (2005) and Marinos (2017).

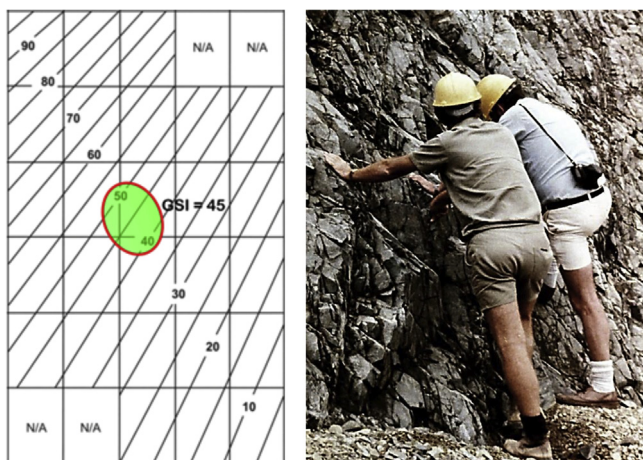


Fig. 10. Interlocking angular Andesite blocks defined by several joint sets, exposed in an open pit mine bench. GSI is fully applicable in this situation and on this scale.

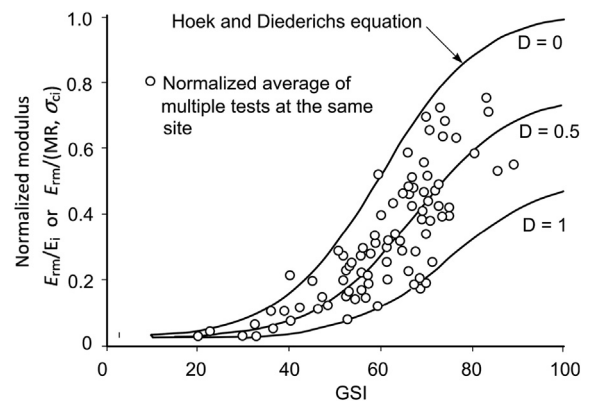


Fig. 13. Plot of normalized in situ rock mass deformation modulus from China (including Taiwan) against Hoek and Diederichs (see Eq. (9)). Each data point represents the average of multiple tests at the same site in the same rock mass.

Table 2 sets out several examples in which the method of excavation and the control of blasting are of great importance. In the case of tunnels, this is particularly important since the limited

amount of space available in a tunnel means that any failure can have a serious impact on the excavation schedule and cost and even on the performance of the final tunnel. Careful excavation by a well-

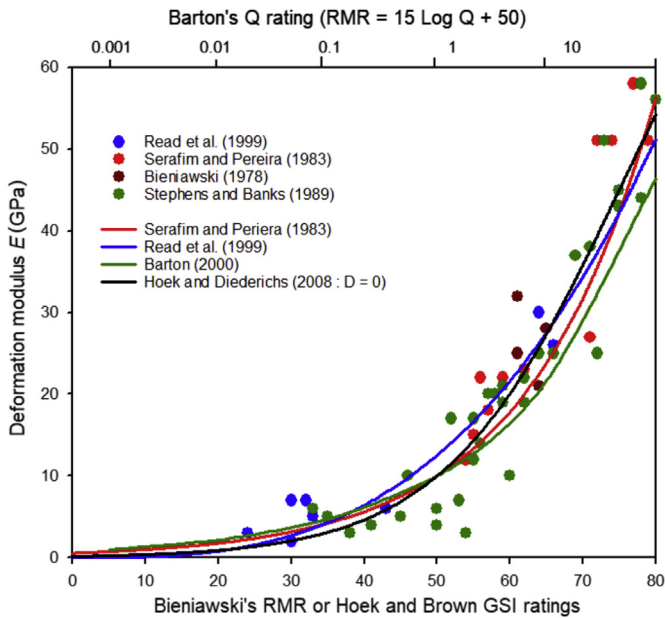


Fig. 14. Comparison between field measurements and deformation modulus values predicted by several authors.

chosen tunnel boring machine (TBM) or road-header can reduce many of these problems. However, in a drill-and-blast tunnel, the blasting design and execution is of critical importance.

A common error is to assume that the disturbance factor  $D$  should be applied to the entire rock mass in which the excavation is conducted. This will result in an extremely conservative and inappropriate design.

The first illustration in Table 2 shows a tunnel in which the blast-hole pattern, explosive charges, and detonation sequence have all been carefully designed and executed. Of importance is the careful control of the drillhole alignment for the ultimate smooth blast used to create the tunnel walls. In this case, the disturbance factor  $D = 0$  can be used with confidence since there is minimal damage to the surrounding rock mass.

A more complex situation is illustrated in the second photograph in Table 2, showing a tunnel excavated by the top heading and bench method. Unless the displacements induced by the excavation of the lower bench are controlled by the placement of an invert strut, excessive displacements in the lower part of the tunnel can result in significant rock mass failure. In this case, a disturbance factor of  $D = 0.5$  is considered appropriate for the rock mass in which the lower half of the tunnel is excavated. Note that this damage factor should only be applied to a zone of about 2 m width around the bottom half of this 12 m span tunnel.

An example of a very poorly designed and executed tunnel blast is shown in the third illustration in Table 2. Poor drillhole alignment control and lack of attention to the blast design and detonation sequence have resulted in damage to the rock walls. A disturbance factor of  $D = 1.0$ , with a linear decrease to zero, has been assigned to the first 3 m of the rock mass surrounding this 8 m span tunnel.

The fourth illustration in Table 2 shows a 15 m high slope in a dam spillway in which pre-split blasting has been used to create the face on the left. Relaxation of the face can still occur and a blast disturbance factor of  $D = 0.5$  has been assigned to 1–2 m of rock behind this face. The rock mass on the right has been mass blasted with little control of the drillhole spacing and alignment of the charges and detonation sequence. The most severe disturbance

factor of  $D = 1.0$  has been assigned to 2–3 m of the rock mass behind this slope.

The final illustration in Table 2 shows a very large open pit with slopes approaching 1000 m in total height. Several different disturbance factors must be considered in this example. It is important to differentiate between slopes created during active mining and the final design slopes which are required to remain stable for many years. During active mining, the blasting is required to produce large volumes of uniformly fragmented ore to meet the requirements of ore processing for mineral extraction. On the other hand, the final slopes are required to remain stable to ensure access to the ore and safe and efficient disposal of the waste.

Individual 18 m high benches will generally have suffered significant damage because of their proximity to the production blasts required for removal and fragmentation of the ore. A disturbance factor of  $D = 1.0$  is assigned to the rock immediately behind these benches. This disturbance factor can be graded downward, to a final value of  $D = 0$ , as the distance behind the face increases to about 30% of the slope height.

The inter-ramp and final slopes will also have suffered stress relaxation damage which can exceed the effects of blasting in large excavations. Rose et al. (2018) state that: "Selection of an appropriate range of depth or stress defining the disturbance transition requires consideration of whether slope stability conditions are dominated by geologic structure, rock mass conditions, groundwater, in situ stresses, slope geometry, poor blasting, or a combination of these factors." They have developed a disturbance rating for open pit mine slopes which can provide guidelines for the selection of the depth of the fully disturbed conditions behind the slope and the decrease in the damage factor  $D$  over a range of slope heights.

While much smaller blasts are used for slopes for roadcuts, dam spillways and foundation excavations, the application of the damage factor should be like that applied in open pit mining. However, the overall factor of safety of the design may be higher than that for open pit mine slopes to accommodate the longer life expectancy.

## 9. The overall design process

Having set out all the input data required for a full analysis using the Hoek–Brown failure criterion and GSI system, it is useful to consider the full sequence of data acquisition, interpretation, utilization, and back analysis. Fig. 15 is a flow chart in which the sequence of data acquisition from laboratory tests and field observations are combined to calculate the principal stress relationship for a rock mass. This is followed using analytical or numerical models to produce an excavation design which is then implemented, and its performance monitored by convergence measurements.






A final step is the back analysis of the monitoring results and the feed-back of the results of this analysis into the early stages of the flow chart. This step is critical since it is the only means whereby the design method and the input parameters used in the calculations can be validated. Back analysis should be an ongoing process throughout and even after the construction process so that adjustments and corrections can be made at all stages. This provides not only confidence in the design but also information which can be used to improve on the determination of input parameters and the design methodology.

## 10. Determination of intact rock strength properties

The starting point for the procedure outlined in the flow chart in Fig. 15 is the determination of the intact rock properties. This involves laboratory uniaxial and triaxial tests on carefully collected and prepared rock core samples. Generally, care is taken to ensure



**Table 2**  
Guidelines for estimating disturbance factor  $D$  due to stress relaxation and blasting damage.

The disturbance factor $D$ should never be applied to the entire rock mass surrounding an excavation		
Appearance of rock mass	Description of rock mass	Suggested value of $D$
	Excellent quality-controlled blasting or excavation by a road-header or tunnel boring machine results in minimal disturbance to the confined rock mass surrounding a tunnel. The blasting design for this tunnel is discussed in <a href="http://www.rocsience.com/assets/resources/learning/hoek/Practical-Rock-Engineering-Chapter-16-Blasting-Damage-in-Rock.pdf">http://www.rocsience.com/assets/resources/learning/hoek/Practical-Rock-Engineering-Chapter-16-Blasting-Damage-in-Rock.pdf</a>	$D = 0$
	Mechanical or manual excavation in poor quality rock masses gives minimal disturbance to the surrounding rock mass. Where squeezing problems result in significant floor heave, disturbance can be severe unless a temporary invert, as shown in the photograph, is placed.	$D = 0$ $D = 0.5$ with no invert
	Poor control of drilling alignment, charge design and detonation sequencing results in very poor blasting in a hard rock tunnel with severe damage, extending 2 or 3 m, in the surrounding rock mass.	$D = 1.0$ at surface with a linear decrease to $D = 0$ at $\pm 2$ m into the surrounding rock mass
	Small-scale blasting in civil engineering slopes results in modest rock mass damage when controlled blasting is used, as shown on the left-hand side of the photograph. Uncontrolled production blasting can result in significant damage to the rock face.	$D = 0.5$ for controlled presplit or smooth wall blasting with $D = 1.0$ for production blasting
	In some weak rock masses, excavation can be carried out by ripping and dozing. Damage to the slopes is due primarily to stress relief. Very large open pit mine slopes suffer significant disturbance due to heavy production blasting and stress relief from overburden removal.	$D = 0.7$ for mechanical excavation effects of stress reduction damage $D = 1.0$ for production blasting A transitional $D$ relationship incorporating the effects of stress relaxation can be derived from the disturbance rating*

Note: \*A disturbance rating for open pit slopes has been published by Rose et al. (2018).

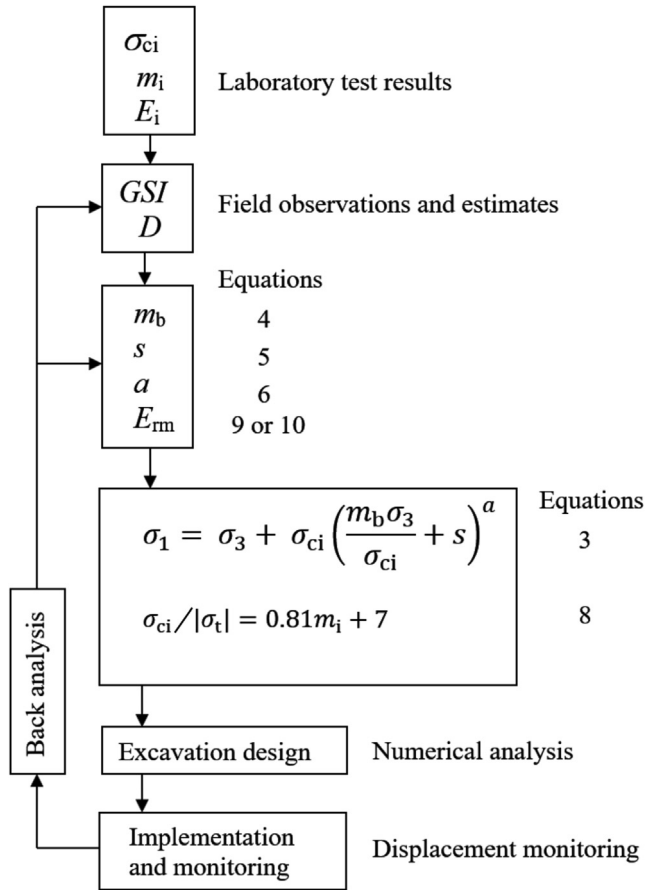


Fig. 15. Flow chart for the application of the Hoek–Brown criterion and GSI system to an excavation design.

that the core is recovered from homogeneous rock in which failure will occur through intact rock material. These samples are tested using current standard and suggested methods outlined in the ISRM suggested methods (Ulusay and Hudson, 2007).

When the Hoek–Brown criterion was introduced, it was recommended that triaxial test results should be analysed by linear regression of the following version of Eq. (1) (Hoek, 1983):

$$(\sigma_1 - \sigma_3)^2 = m_i \sigma_{ci} \sigma_3 + \sigma_{ci}^2 \quad (11)$$

This approach was used for several years until it was realized that the method was inadequate for the analysis of data other than closely spaced points with very little scatter about a general trend line. A variety of methods are available for fitting curves through non-uniform distribution of triaxial test data. One of these, known as the modified Cuckoo search (Walton et al., 2011), is included in the Rocscience program RocData which can be used for the interpretation of laboratory test data.

Bozorgzadeh et al. (2018) and Contreras et al. (2018) used Bayesian statistics to quantify the uncertainty of intact rock strength. This approach provides an alternative to conventional probabilistic or frequentist methods such as those described above. To deal with the problem of outliers in sets of test data for rock, Contreras et al. (2018) use Student's *t* distribution in place of the commonly assumed normal distribution as a starting point in the analysis. The difference between these two distributions, for a hypothetical but not unrealistic data set, is illustrated in Fig. 16 in which the impact of a single outlier is evident.

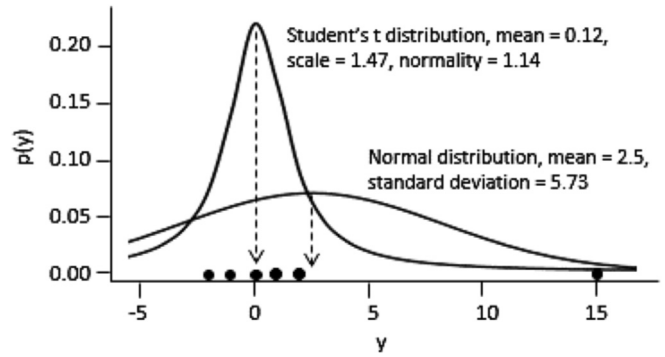


Fig. 16. Comparison between a normal distribution and Student's *t* distribution for the analysis of a small data set with an outlier (after Kruschke, 2015).

Fig. 17 is a plot of the results obtained from a Bayesian analysis of a triaxial data set, giving an unconfined compressive strength of σ<sub>ci</sub> = 114.5 MPa and m<sub>i</sub> = 11.5. For comparison, the result given by the RocScience RocData modified Cuckoo nonlinear regression analysis with absolute residuals is σ<sub>ci</sub> = 116.2 MPa and m<sub>i</sub> = 10.6, which has also been plotted in Fig. 17. In this case, the differences between the Bayesian analysis and the nonlinear regression analysis are not large. As Bozorgzadeh et al. (2018) demonstrated, the advantages of their novel Bayesian regression analysis technique become more apparent for sparser and more widely scattered data sets.

In estimating the σ<sub>ci</sub> of intact rock, an important issue is the size of the rock block under consideration, as compared to the strength determined from laboratory tests on 50 mm core samples. Fig. 18, published by Hoek and Brown (1980a), includes the results of laboratory tests on a wide range of rock types and specimen sizes. The trend shown in this plot is typical of that suggested by the reasoning that the greater the volume of rock, the greater the probability that a larger number of defects are available for the formation of through-going failures. This trend should be kept in mind when estimating the σ<sub>ci</sub> of in situ rock blocks.

In the preceding discussion, it has been assumed that the intact rock specimens are homogeneous and isotropic and that the values of the unconfined compressive strength σ<sub>ci</sub> and the constant m<sub>i</sub> are representative of the intact rock in the blocks of the rock mass. In fact, this assumption is not always valid since in many rock masses, defects such as veins, micro-fractures and weathered or altered components can reduce the intact rock strength. Ideally, tests should be carried out on specimens large enough to include representative sections containing these defects, but collection and preparation of such specimens can be challenging.

In discussing rock mass classifications, such as GSI, Day et al. (2012) described the blocks, defined by intersecting joints, as interblock structures. They defined the veins, stockwork and other defects as intrablock structures and pointed out that these should also be considered in the rock mass characterization since they have a significant influence on intact rock strength. They suggested that the defects in both the interblock and intrablock structures can be incorporated into the GSI classification.

Day et al. (2012)'s suggestion is illustrated in Fig. 19 in which the influence of size is considered in determining the use of GSI. The starting point for this chart is a typical intact rock core, but there is no reason why this starting point should not be the intrablock structure within the core as suggested by Day et al. (2012). They emphasized that the reduction of the intact rock strength by this method must be carried out with care to avoid over-penalization of the rock mass strength.

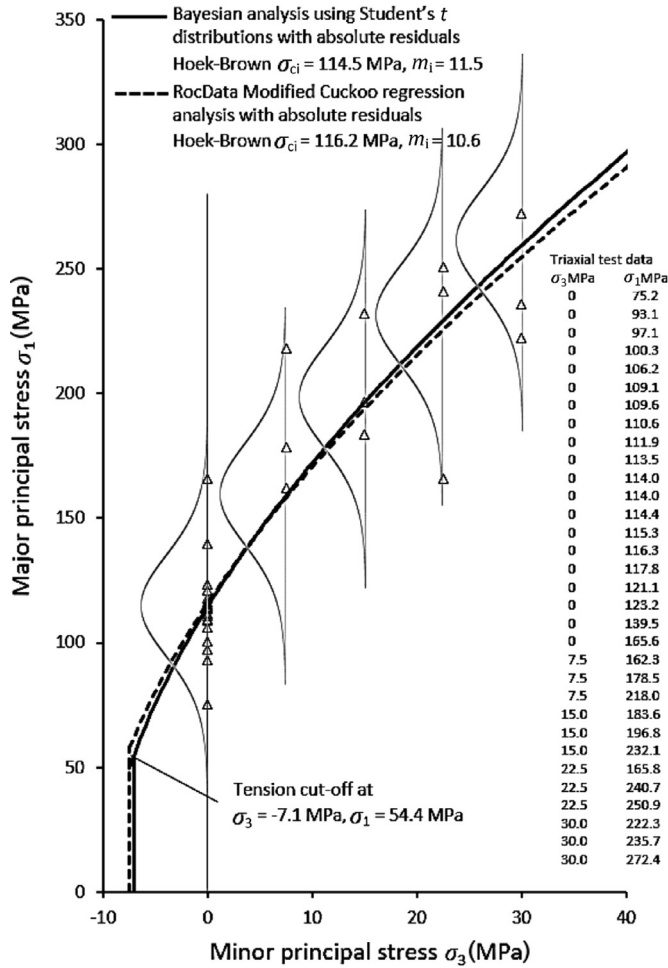


Fig. 17. Analysis of triaxial tests on Coburg limestone using a Bayesian analysis incorporating Student's *t* distribution, compared with an analysis using the RocData modified Cuckoo method.

Bewick et al. (2015, 2019) and Kaiser et al. (2015) have examined the issue of veins and microfractures in intact rock core or blocks. Their emphasis is on the effects of these veins and micro-fractures on rock mass classification and rock block strength. As noted in Section 5, these authors have proposed that, for sparsely jointed hard rock with a GSI rating of greater than 65, Eqs. (4)–(6) may require modification to reduce the strength of rock masses under high in situ stress conditions.

Weathering, alteration and deterioration of the core in storage are factors that need to be considered during collection and preparation of rock specimens. An example of the deterioration of mudstones and siltstones due to changes in moisture content during storage is illustrated in Fig. 20. In such cases, care needs to be taken to seal the core during transportation and storage or, in extreme cases, to carry out the strength tests on site as soon as possible after core recovery. In the example illustrated, immediate sealing of excavated surfaces with shotcrete was necessary to preserve the rock mass strength.

The triaxial cell, illustrated in Fig. A1 in the Appendix, was originally designed to permit triaxial testing of rock specimens, such as those illustrated in Fig. 20, on drilling sites.

### 11. Practical application of the GSI characterization

The starting point for any site investigation program is a good geological model of the site. Ideally, this model should be

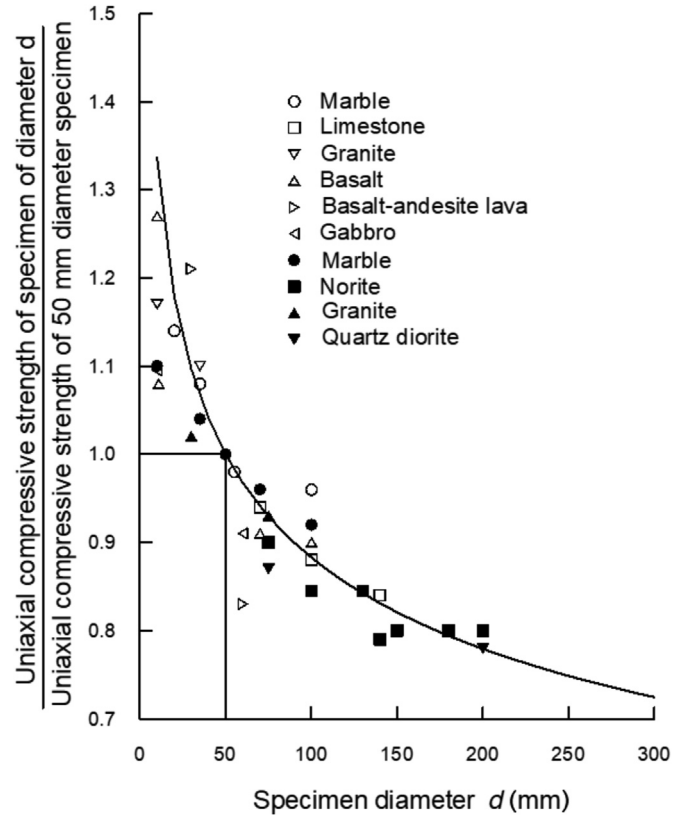


Fig. 18. Influence of specimen size on the UCS of intact rock, compared to that of a 50 mm diameter core sample (after Hoek and Brown, 1980a).

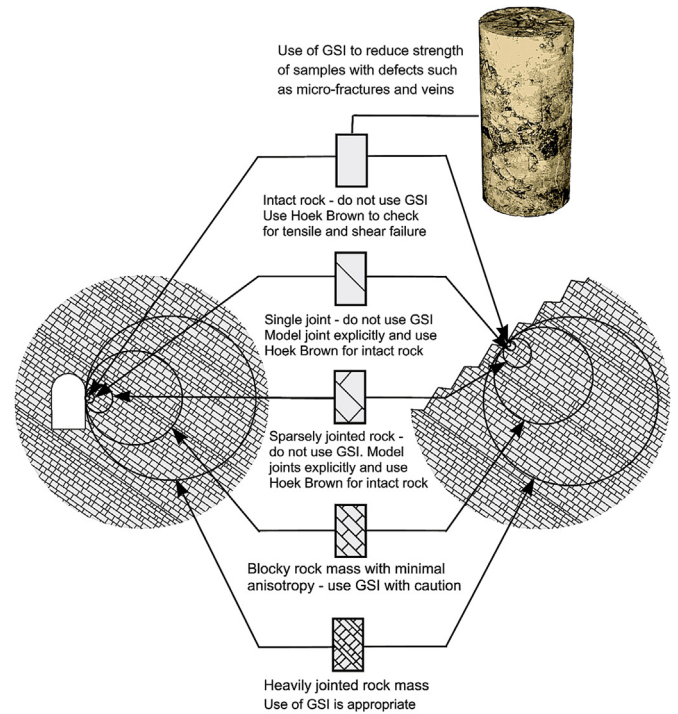


Fig. 19. Size effects in rock mass characterization. Modified after Hoek and Brown (1980a).

constructed by local geologists who have familiarity with the regional geology and experience in working with the rock types encountered on the site. Without such a model, the application of



Fig. 20. Core of sandstone, siltstone and mudstone immediately after recovery (left) and after several months of storage in a core shed (right).

GSI can become a confusing array of numbers being manipulated by engineers anxious to obtain input for analytical or numerical models.

The GSI characterization scheme was devised for engineering geologists and geologists who can utilize all the information contained in the chart presented in Fig. 7 to arrive at a range of probable GSI numbers for each rock unit. As for the case of triaxial test data obtained from laboratory testing, discussed in Section 10, the range of GSI values should also be treated as a distribution. Langford and Diederichs (2015) and Contreras and Brown (2018) advocated that the same statistical processes should be applied to both the intact rock properties and the GSI estimates to provide the ranges of the final rock mass properties chosen for design.

Many projects have been completed successfully using a deterministic approach in which the mean values for intact rock properties and GSI are chosen and applied to the design process outlined in Fig. 15. This approach is acceptable when it is associated with a well-planned rigorous back analysis program and where the contract can accommodate the changes which are necessary to utilize the information from this back analysis. Examples of this type of approach are presented in the next sections.

The GSI system assumes that, because the rock mass is made up of a sufficiently large number of joint sets and randomly oriented discontinuities, it can be treated as a homogeneous and isotropic mass of interlocking blocks. Failure of this rock mass is the result of sliding along discontinuities or rotation of blocks, with relatively little failure of the intact rock blocks. The ideal rock mass for which GSI was originally developed is a heavily jointed rock mass with high intact rock strength, such as that illustrated in Fig. 1.

Fig. 19 shows that the ratio of the size of the blocks to the size of the structure in which they exist is an important factor to be considered when deciding whether GSI should be used. For example, in the face of a 10 m span tunnel, an average joint spacing of 0.5 m would result in about 400 blocks being exposed in a square mine tunnel or about 315 blocks in a circular tunnel. This would be considered a reasonable scale for the application of GSI. The same GSI rating would be applied to smaller blocks with similar geometry. It is the shape of the blocks and the characteristics of the discontinuities which separate them, rather than their size, that controls their

interlocking behaviour. In this example, joint spacings of 2 m or more would result in fewer than 25 blocks which, as shown in Fig. 9, would result in the failure of individual blocks rather than the overall failure of a jointed rock mass. GSI should not be used in this case.

In a 100 m high rock slope, a blocky rock mass with an average joint spacing of 3 m would expose about 1000 blocks in a 100 m length of the slope. This would qualify for a condition in which GSI could be applied. On the other hand, 15 m high benches in the same rock mass would not qualify since only about 25 blocks would occur in a 15 m length of the slope.

In cases where GSI is not applicable, the failures will be controlled by the three-dimensional geometry of the intersecting features in the rock mass. Stability analyses in these cases should be carried out using tools that are available for calculating the factors of safety of sliding blocks or wedges.

Many of the applications and limitations of the GSI were discussed by Marinou and Hoek (2000) and Marinou et al. (2005). Users who are not already familiar with the GSI system are advised to read these papers before embarking on applications in the field. The following three case histories have been chosen to illustrate the practical application of the Hoek–Brown criterion and the GSI system in a variety of geological environments and project settings.

## 12. The Driskos tunnel on the Egnatia Highway

The 670 km long Egnatia Highway across northern Greece has 77 twin tunnels of almost 100 km in total length. These 12 m span tunnels pass through complex geological conditions in a converging rim between the European and African plates. Many unfavourable geotechnical environments occur along the highway route leading to difficult tunnelling conditions. One of the tunnels on this route is the Driskos tunnel, which will be discussed in this example.

Between 1998 and 2006, Dr. Evert Hoek and Professor Paul Marinou formed a Panel of Experts to advise Egnatia Odos S.A. the company set up to manage the construction of the project, on geotechnical issues related to tunnel design and construction. In 2000, they reviewed the design of the 4.6 km long Driskos tunnel. A longitudinal profile along the tunnel, depicting the geological formations, is presented in the upper half of Fig. 21.

Based on their knowledge of the regional geology of the area and the site investigations that had been carried out, they estimated the GSI values along the tunnel route and calculated the percentage strain which could be anticipated. These percentage strains are plotted along the tunnel in the lower graph in Fig. 21.

The largest strains were anticipated in a section of very poor-quality flysch at the deepest central section of the tunnel. A typical outcrop of this flysch, a tectonically deformed sequence of sandstones, siltstones and mudstones, is illustrated in Fig. 12.

Hoek and Marinou (2000) developed a method for estimating the strain, defined as the ratio of tunnel closure to tunnel diameter  $\times 100$ , for a tunnel subjected to in situ stresses sufficiently high to cause squeezing.

To carry out the calculations of strain, an estimate of the rock mass strength is required, and this can be made using the approximation given for line 6 in Fig. 22. A comparison between this estimate and estimates made by other authors and in situ test results shows acceptable agreement for values of GSI up to 65.

In the case of the Driskos tunnel, the in situ stress  $p_0$  is assumed to equal the product of the depth of the tunnel and the unit weight of the rock mass. The calculated percentage strains, for the lowest and highest GSI estimates, are plotted along the tunnel alignment

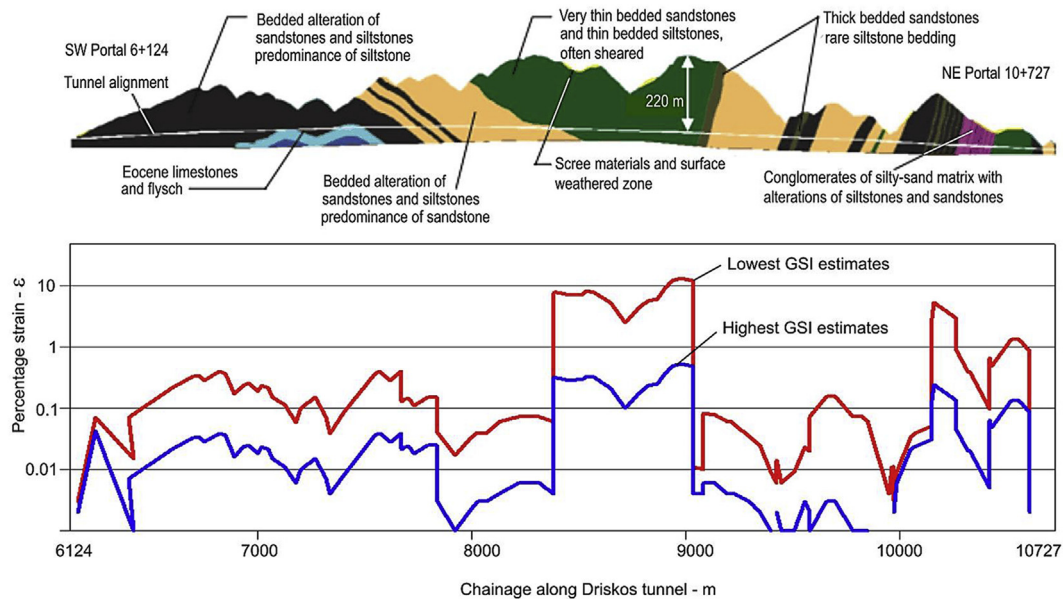


**Fig. 21.** Longitudinal profile along the Driskos tunnel depicting the geological formations encountered and the predicted percentage closure strain in these sections. Adapted from Vlachopoulos et al. (2012).

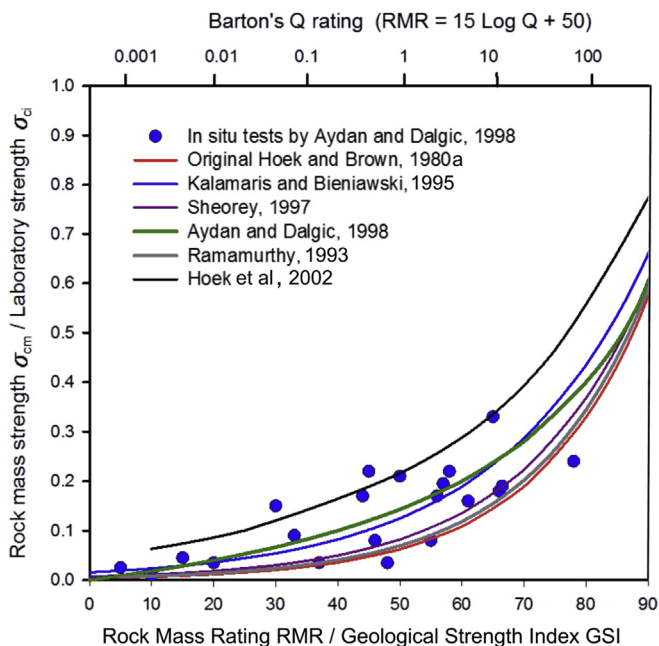


**Fig. 22.** Approximate relationship between the ratios of rock mass to laboratory unconfined compressive strength for a range of RMR or GSI values. (Von Kármán, 1911, Ros et al., 1928, Rosengren and Jaeger, 1968, Franklin and Hoek, 1970, Kovari and Tisa, 1974, Gerogiannopoulos and Brown, 1978, Ramamurthy, 1993, Kalamaris and Bieniawski, 1995, Sheorey, 1997, Aydan and Dalgic, 1998).

in Fig. 21, which shows that strains of the order of 10% were anticipated for the lowest GSI values, for a section of the Driskos tunnel between approximate chainages of 8300–9000. During the tunnel construction, significant strains occurred in the tunnel in this zone and the installed steel sets, rockbolts and shotcrete proved to be inadequate to prevent the deformation from encroaching on the space required to accommodate the final lining. Additional tensioned cables had to be installed to provide the support required to stabilize the tunnel.

The relationship, proposed by Hoek et al. (2002), is used to calculate the strain for different ratios of rock mass strength to in situ stress as shown in Fig. 23. A comprehensive retrospective analysis of the Driskos tunnel design and construction issues is given by Vlachopoulos et al. (2012).

### 13. The Ingula underground powerhouse project

The Ingula Pumped Storage Project in South Africa comprises two reservoirs interconnected by a tunnel system, with reversible pump/turbine units with a total rated generation capacity of 1332 MW located in an underground powerhouse complex. This complex consists of a 26 m span machine hall, a transformer hall with a 19 m span, 11 m diameter busbar tunnels, 5 m diameter high pressure penstocks, a 9 m diameter main access tunnel and a series of smaller adits and shafts. It is located at a depth of almost 400 m below ground level. The 184 m long machine hall has a double curvature profile roof with a relatively low span to height ratio of 2.5 and is up to 50 m deep in the turbine pits. A photograph of the partially completed underground powerhouse cavern is reproduced in Fig. 24.

The Ingula power caverns were constructed under a prominent mountain ridge off the Drakensberg escarpment between the Free State and KwaZulu Natal provinces, South Africa, in the Volksrust Formation of the Ecca Group, Karoo Supergroup which comprises horizontally bedded siltstones, mudstones, and carbonaceous mudstones. The intact rock UCS properties derived from field and laboratory testing are presented as normal distributions in Fig. 2.

In situ stresses were measured in hydro-fracture tests in boreholes and in a small number of overcoring tests. The major horizontal stress is greater, and the minor horizontal stress is slightly lower, than the estimated vertical overburden stress. Hydro-fracture tests at cavern level gave a horizontal/vertical stress ratio of 0.5–0.9, while overcoring tests indicated a ratio of approximately 1.0 in the powerhouse area.

In the design of the Ingula underground powerhouse complex, the conventional deterministic method of combining the Hoek–Brown  $\sigma_{ci}$  and  $m_i$  parameters was used, with GSI values

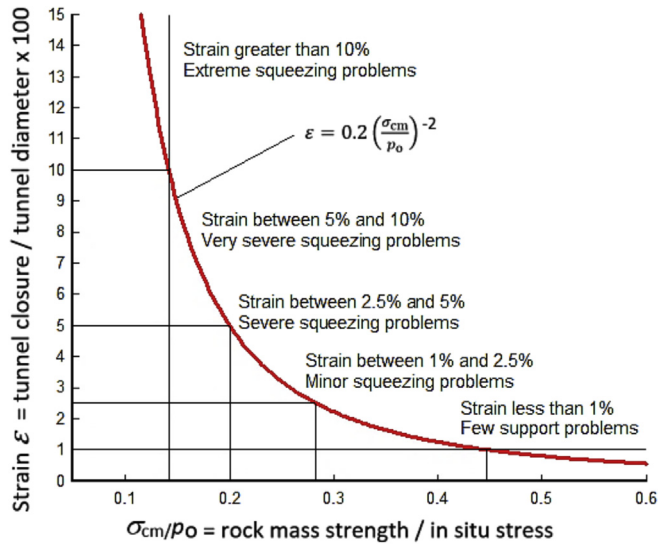


Fig. 23. Percentage strain as a function of the ratio of rock mass strength to in situ stress (Hoek and Marinos, 2000).



Fig. 25. The east slope of the Chuquicamata mine in 2013.



Fig. 24. The 26 m span, 50 m high Ingula underground powerhouse cavern after excavation of bench 3. Photograph provided by G. Keyter and reproduced with permission of ESKOM South Africa.

determined in the field to estimate rock mass strengths for different rock units. The final successful design and construction of the excavations were well documented by Keyter et al. (2008) and Kellaway et al. (2010), which provided an excellent record of this case history.

Initial geological and geotechnical investigations for the Ingula Pumped Storage Project commenced with borehole drilling in 1999. The main phases of the surface geotechnical investigation, the drilling of additional boreholes, and an exploration tunnel were completed in 2005.

The preliminary design of the Ingula underground powerhouse complex was based on the experience gained during the design and construction of the Drakensberg Pumped Storage Project, a sister scheme commissioned in 1981 (Bowcock et al., 1976). At the time of the design of this project, worldwide experience in the construction of underground powerhouse complexes was very limited. After a careful review of three published case histories, the trapezoidal roof arch in the Poatina Project in Tasmania, commissioned in 1964 (Endersbee and Hofto, 1963), was adopted for the Drakensberg

project. Since the Drakensberg powerhouse cavern was the first major underground civil engineering cavern to be constructed in South Africa, full-scale tests of the cavern arch and the concrete lined pressure tunnel were carried out to confirm the support design assumptions. These tests were very successful and provided the information required to complete the design which was successfully implemented in the construction of the underground complex.

Determinations of the deformation moduli of the in situ rock masses in the Drakensberg project were carried out by means of plate bearing tests and by back analysis of the deformations measured in the full-scale tests described above. A surprising result was that the in situ deformation moduli were close to the values determined from laboratory tests on intact samples. This suggested that under the confined stress conditions around the excavations, the rock masses were behaving as very tightly interlocked blocky structures which, in today's terms, would have to be assigned a very high GSI value. Note that the tendency of the mudstones and siltstones, as illustrated in Fig. 20, to disintegrate upon prolonged exposure to air was remedied by the immediate application of shotcrete to all excavated faces. This sealed the rock masses from exposure and preserved the intact properties very effectively.

In designing the underground caverns for the Ingula Pumped Storage Project, the rock mass behaviour in the Drakensberg project was considered, and the interbedded mudstones and siltstones were treated as intact rock with weak horizontal bedding planes. Since this was an unusual design assumption, the designers were reluctant

to assign a GSI value of 100 to the siltstone and mudstone units. Therefore, it was decided to use  $GSI = 70$  in the design process.

Two-dimensional finite element models, set up during the detailed design of the cavern excavation and support, were revised towards the end of the main power cavern excavation to account for the actual geology encountered, excavation sequence, support installation, and convergence information collected during construction. The results of these analyses confirmed that, in fact, the in situ mudstones and siltstones should have been assigned a GSI value of 100. A detailed description of the comparison between the original design assumptions and the values obtained from the post-construction back analysis is presented in a comprehensive paper by Kellaway et al. (2010).

This example illustrates the fact that, in many cases, engineers tend to underestimate the capacity of rock masses when tightly confined by the stress field surrounding underground excavations. Kaiser et al. (2015) examined this issue in detail for highly stressed brittle rocks. They conclude that:

*“Common use of currently available rock mass characterization systems tends to underestimate the strength of highly stressed brittle and often defected rock. It is demonstrated that this is primarily related to flawed interpretation of rock mass characteristics derived from boreholes and laboratory tests without proper consideration of, for example, GSI applicability, laboratory test results failure mode sorting, and failure modes of rock in underground settings.”*

Similar comments can be made for weaker rocks, such as the mudstones and siltstones discussed in the example of the Ingula Pumped Storage Project. In particular, the tendency for these rocks to slake when removed from the in situ environments, can lead to significant underestimation of the rock mass properties.

In the case of the Ingula Pumped Storage Project, the back analysis of a carefully investigated and well-designed project provides a valuable example of the additional information that can be gained on completion of the project. Sakurai (2017) emphasized: *“Field measurement data are only numbers unless they are properly interpreted. Therefore, the most important aspect of field measurements is the quantitative interpretation of measurement results”*.

#### 14. Chuquicamata mine slope stability analysis and conveyor transfer chamber design

The Chuquicamata mine in northern Chile has one of the largest open pits in the world, measuring approximately 4 km long, 3 km

wide, and 1 km deep. Removing ore and waste from the mine on conveyors or by truck, using the haul roads such as that illustrated in Fig. 25, is a complex and expensive process. Hence, planning started more than 10 years ago for a transition from open pit to block caving underground as the mining method (Olavarría et al., 2006). The transition is currently scheduled to occur in 2019 (see Flores and Catalan, 2019).

For many years, the ore has been transported to the surface by means of a conveyor installed in a tunnel behind the East Wall slope. The conveyor has been extended downwards as the depth of the pit increased and, due to limits in conveyor belt lengths, a transfer station was installed in the conveyor tunnel in 2005.

Progressive deepening of the open pit has resulted in ongoing displacements in the East Wall and in the rock mass surrounding the conveyor transfer chamber. This resulted in the need for detailed monitoring of the cavern deformations and periodic adjustment of reinforcement cable tensions and, in some cases, installation of replacement cables. It is important that this chamber remains stable until it is decommissioned when the open pit mining is completed.

In 2012, a review of the conveyor transfer chamber was set up by the mine management. This review was monitored by Dr. E. Hoek, a member of the mine's Technical Advisory Board. The detailed analysis was carried out by P. Varona of Itasca and Dr. F. Duran of the Chuquicamata Geotechnical Department.

An important component of this analysis was the establishment of the rock mass model to be used in numerical models of the slope and chamber. This was based on the results of a geotechnical characterization program initiated by Dr. E. Hoek and Dr. J. Read, members of the first Technical Advisory Board established in 1992. This program involved laboratory testing of intact samples and joints in the seven major rock types surrounding the open pit, as well as 185 km of borehole core logging and 195 km of bench mapping. The results of this geotechnical characterization program, agreed upon by the mine's geotechnical department and approved by the Technical Advisory Board, are summarized in Table 3.

The second important component of the analysis was the existence of a very sophisticated slope displacement monitoring program based on more than 1000 prisms located in sensitive areas of the pit, measured automatically at frequent intervals by electro-optical measuring devices. Information is telemetered to a central monitoring station for interpretation. The locations of the most important prisms around the entrance of the access tunnel to the conveyor transfer station are shown in Fig. 26.

In addition, several radar displacement monitoring units, such as that illustrated in Fig. 27, are available on the mine. One of these was deployed to monitor the displacements of the slope in which

**Table 3**  
Rock mass and discontinuity properties.

Rock mass properties	UCS (MPa)	$\gamma$ (t/m <sup>3</sup> )	Distribution of GSI			$m_i$
			Minimum	Mean	Maximum	
Fortuna granodiorite (GDF)	110	2.59	29	46	63	20
Moderate shear zones (ZCM)	50	2.47	30	40	56	22
Intense shear zones (ZCI)	7.5	2.31	13	25	51	22
Brecciated shear/faults (BEF)	25	2.51	15	25	35	20
Sericite with high quartz ( $Q > s$ )	60	2.67	46	60	70	25
Sericite with similar quartz ( $Q = s$ )	40	2.63	37	47	55	14
Sericite with low quartz ( $Q < s$ )	20	2.59	27	34	49	15.5
Discontinuity properties	Friction angle (°)			Cohesion (kPa)		
	Minimum	Mean	Maximum	Minimum	Mean	Maximum
Structure	16	18	20	10	20	30
West fault	22	25	28	30	40	50

the transfer chamber is located. A radar image of displacements in the east face of the mine is reproduced in Fig. 28.

Analysis of the slope displacements, measured by both the electro-optical system and the radar unit, demonstrated that the displacements in a zone in the rock mass surrounding the transfer chamber were significantly larger than those in the remainder of the East Wall. This suggested that a wedge, bounded by major structural features shown by blue lines in Fig. 26, had formed in the rock mass and was moving more than the surrounding rock mass in both the face of the east slope and that surrounding the transfer chamber. This model incorporated the joint-defined rock blocks with rock mass strength and deformation properties defined by the Hoek–Brown criterion and GSI parameters given in Table 3. The major structural features were assigned strength properties defined by the discontinuity property values listed in Table 3. The cable reinforcement installed from the transfer chamber, as shown in Fig. 29, was included in the model illustrated in Fig. 30.

During the 2012 review, a 3D discrete element model, using the Itasca 3DEC program, was created to study the displacements and

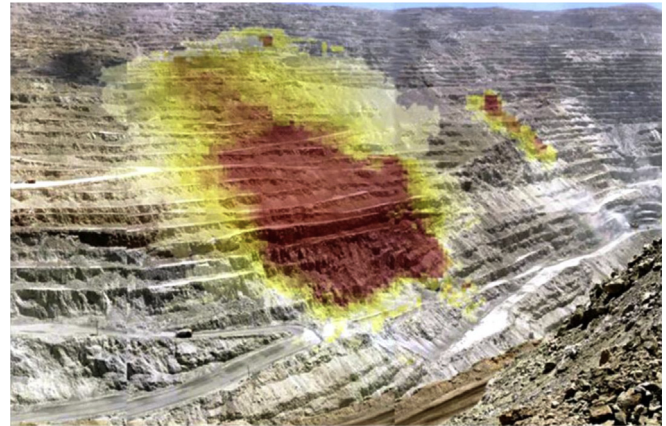


Fig. 28. Radar image showing displacements in the east face. The transition from yellow to red colors indicate increasing displacements in the rock mass.

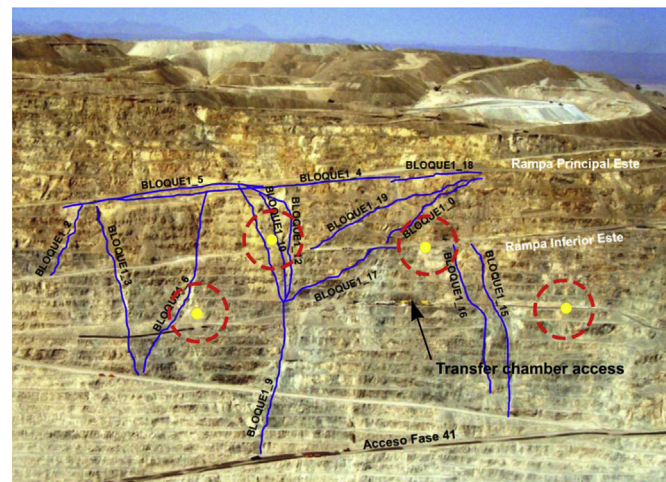


Fig. 26. View of the east face of the Chuquicamata mine showing the location of the conveyor transfer chamber, major structural features and the location of critical optical distance measurement targets (yellow spots circled in red).



Fig. 27. Radar equipment for monitoring slope displacements.

rock mass behaviours in both the face of the east slope and that surrounding the transfer chamber. This model incorporated the joint-defined rock blocks with rock mass strength and deformation properties defined by the Hoek–Brown criterion and GSI parameters given in Table 3. The major structural features were assigned strength properties defined by the discontinuity property values listed in Table 3. The cable reinforcement installed from the transfer chamber, as shown in Fig. 29, was included in the model illustrated in Fig. 30.

The outcome of this analysis, shown in Fig. 31, was that the deformation results, for both the slope face and the transfer chamber, were in acceptable agreement with the monitored values. This provided the Geotechnical Department with a sound basis on which to plan cable reinforcement tension adjustments and cable replacement installations to ensure that the chamber remained stable for the remainder of the open pit operation.

## 15. Conclusions

In the almost 40 years since its introduction, the Hoek–Brown criterion for intact rock and rock masses has gained wide-spread international use for a wide range of engineering applications. The criterion for intact rock was based on brittle fracture concepts

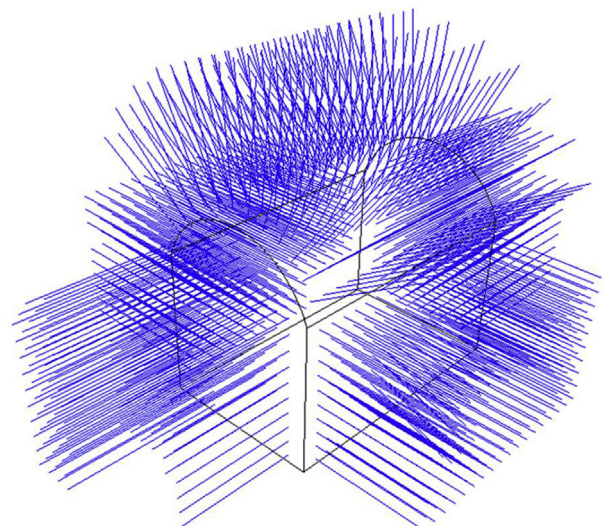


Fig. 29. Cable reinforcement installed from the conveyor transfer chamber. The cavern has a span of 20 m, a height of 25 m and a length of 60 m. Support consists of 15 and 20 m long stressed cables.



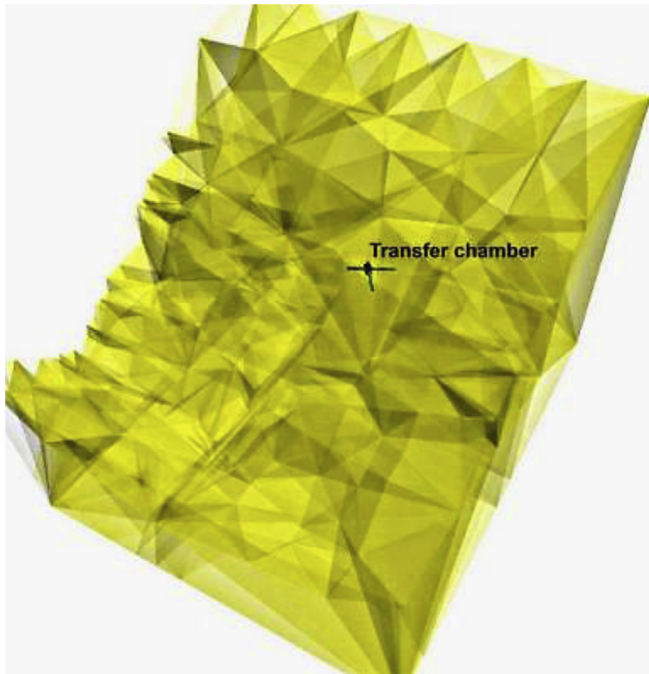


Fig. 30. 3DEC model of the East Wall including the transfer chamber.

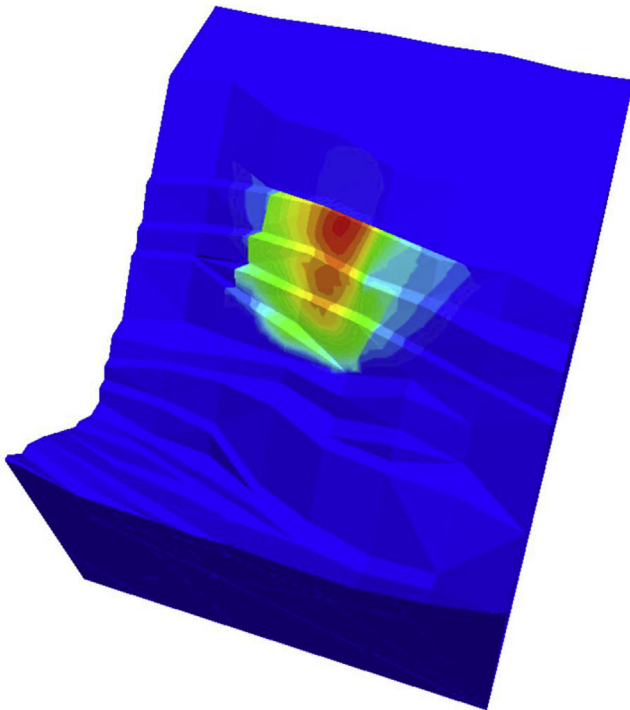


Fig. 31. Displacement contours in the East Wall, generated in a progressively mined 3DEC model. The transition of colours, from blue to red, represent increasing displacements in the rock mass.

and so it should only be used in the brittle behaviour range. Since its introduction, several revisions and updates have been made to the criterion, but its basic form has remained unchanged. A major revision made in the early 1990s accompanied the development of the GSI to quantify engineering geological observations of the structure and condition of rock masses.

The present update emphasizes the intended application of the criterion to the brittle fracture of intact rock; expands on the previously existing methods of evaluating test results for the mechanical properties of intact rock by applying the Bayesian approach to assess uncertainty; discusses the use of the GSI to describe the structure and condition of a wide range of types of rock masses; expands on the previously published guidelines for the selection of the important disturbance factor,  $D$ ; sets out a recommended sequence of calculations for use in applying the criterion; and illustrates its application to practical rock engineering through three different examples.

Despite the revisions that have been made to the criterion and the experience gained in its use over almost 40 years, care must be exercised in seeking to apply the criterion to some rock masses, particularly those at the higher and lower ranges of GSI. It is essential that the geology of the site be well understood, and that the mechanics of the engineering problems involved be evaluated critically. When this has been done, the methods discussed in this paper may be used to evaluate the parameters in the criterion for the intact rock and the rock mass.

### Conflicts of interest

The authors wish to confirm that there are no known conflicts of interest associated with this publication and there has been no financial support for this work, from any source, that could have influenced its outcome.

### Acknowledgements

The authors wish to express their acknowledgements to organizations and individuals who have provided permission to publish materials in case histories and who have contributed to discussions on the development of the Hoek–Brown creation and the Geological Strength Index. It is impossible to name everyone, but a partial list of organizations includes Egnatia Odos S.A. Greece, the South African Electricity Supply Commission (ESKOM), Braamhoek Consultants Joint Venture (BCJV), the Chuquicamata Division of Codelco, Chile. Individuals who have contributed are Rob Bewick, Ming Cai, Trevor Carter, Carlos Carranza-Torres, Joe Carvalho, Luis-Fernando Contreras, Brent Corkum, Mark Diederichs, Felipe Duran, Davide Elmo, Esteban Hormazabal, Jean Hutchinson, Peter Kaiser, Gerhard Keyter, Tom Lam, Loren Lorig, Derek Martin, Paul Marinos, Vassilis Marinos, Dougal McCreath, Bruno Marrai, Terry Medhurst, Bonnie Newland, Luis Olivares, Stephen Priest, John Read, Laurie Richards, Nick Rose, Peter Stacey, Pedro Varona, Nicholas Vlachopoulos, and David Wood.

### Appendix. Triaxial and tensile testing.

Tensile testing can be introduced into a triaxial test program by means of a modification used by Ramsey and Chester (2004). Instead of inserting a cylindrical specimen into a triaxial cell, they substituted a dogbone specimen as illustrated in Fig. A1. The reduced section of the specimen was wrapped in Plasticine modelling clay. When subjected to triaxial confinement, this modelling clay yields plastically and transmits a uniform pressure onto the curved section of the dogbone specimen. Since the ends of the specimen are larger in diameter than the central test section, a tensile stress is induced in the test section.

If  $d_1$  is the diameter of the core and  $d_2$  the diameter of the reduced test section, the tensile stress  $\sigma_3$  induced along the axis of the specimen, for a confining pressure of  $P$ , is

$$\sigma_3 = P(d_1^2 - d_2^2)/d_2^2 \quad (A1)$$

By adjusting the ratio of the diameters  $D$  and  $d$ , the confining pressure  $P$  and the axial load applied to the specimen, a range of  $\sigma_3$  and  $\sigma_1$  stresses can be generated in the tensile zone, as shown in Fig. A2. The preparation of a dogbone specimen on a lathe is illustrated in Fig. A3.

There is strong justification for using the dogbone specimen, illustrated in Fig. A2, for triaxial testing. This is because the smooth transition of the stresses from the enlarged specimen ends to the central test section reduced the potential for axial splitting, particularly at low confinement, which is common when testing cylindrical specimens loaded by steel plates.

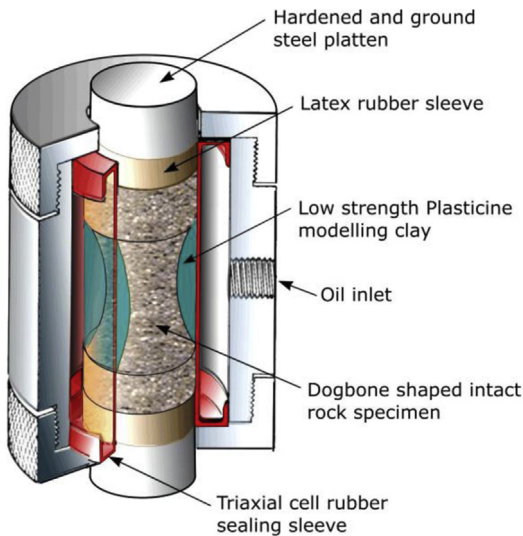


Fig. A1. Triaxial cell with a dogbone specimen for triaxial tensile testing.

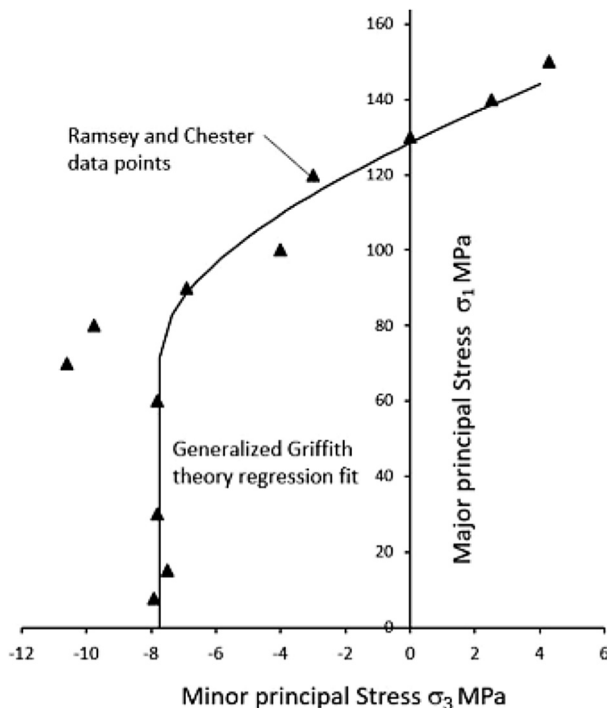


Fig. A2. Plot of triaxial tension data points obtained by Ramsey and Chester (2004).

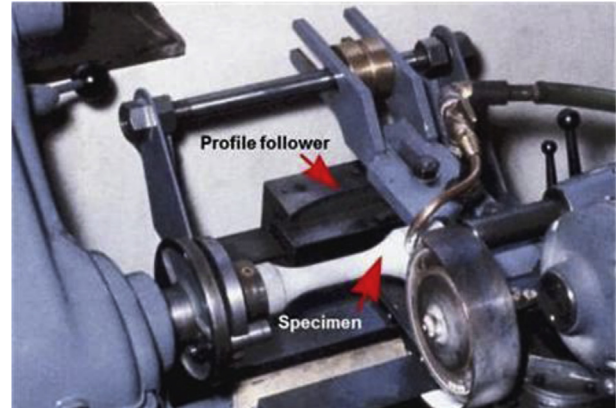


Fig. A3. Preparation of a dogbone specimen using a tool-post grinder attached to a profile follower on a lathe.

## References

- Aydan O, Dalgic S. Prediction of deformation behaviour of 3-lane Bolu tunnels through squeezing rocks of North Anatolian fault zone (NAFZ). In: Proceedings of the regional symposium on sedimentary rock engineering, Taipei, China; 1998. p. 228–33.
- Andrieu GE. Brittle failure of rock materials. Rotterdam: A.A. Balkema; 1995.
- Barton N. Some new Q value correlations to assist in site characterization and tunnel design. International Journal of Rock Mechanics and Mining Sciences 2002;39(2):185–216.
- Bewick RP, Amann F, Kaiser PK, Martin CD. Interpretation of UCS test results for engineering design. In: Proceedings of the 13th international congress on rock mechanics: ISRM congress 2015 – advances in applied & theoretical rock mechanics. Montréal, Canada: International Society for Rock Mechanics; 2015. paper 521.
- Bewick RP, Kaiser PK, Amann F. Strength of massive to moderately jointed hard rock masses. Journal of Rock Mechanics and Geotechnical Engineering 2019;11(3) (in this issue).
- Bieniawski ZT. Determining rock mass deformability – experience from case histories. International Journal of Rock Mechanics and Mining Sciences and Geomechanics Abstracts 1978;15(5):237–47.
- Bobich JK. Experimental analysis of the extension to shear fracture transition in Berea sandstone. MS Thesis. Texas A & M University; 2005.
- Bowcock JB, Boyd LM, Hoek E, Sharp JC. Drakensberg pumped storage scheme: rock engineering aspects. In: Bieniawski ZT, editor. Exploration in rock engineering. Proceedings of the symposium on exploration for rock engineering. Rotterdam: A.A. Balkema; 1976. p. 121–39.
- Bozorgzadeh N, Escobar MD, Harrison JP. Comprehensive statistical analysis of intact rock strength for reliability-based design. International Journal of Rock Mechanics and Mining Sciences 2018;106:374–87.
- Brace WF. Brittle fracture of rocks. In: Judd WR, editor. State of stress in the Earth's crust. New York: Elsevier; 1964. p. 111–74.
- Brown ET. Strength of models of rock with intermittent joints. Journal of the Soil Mechanics and Foundations Division 1970;96(SM6):1935–49.
- Brown ET, Hoek E. Discussion on paper 20431 by R. Ucar entitled "Determination of shear failure envelope in rock masses". Journal of Geotechnical Engineering 1988;114(3):371–73.
- Cai M, Kaiser PK, Uno H, Tasaka Y, Minami M. Estimation of rock mass deformation modulus and strength of jointed hard rock masses using the GSI system. International Journal of Rock Mechanics and Mining Sciences 2004;41(1):3–19.
- Contreras LF, Brown ET. Bayesian inference of geotechnical parameters for slope reliability analysis. In: Slope stability 2018 – XIV international congress on energy and mineral resources. Seville, Spain: Asociación Nacional de Ingenieros de Minas; 2018. p. 1998–2026.
- Contreras LF, Brown ET, Ruest M. Bayesian data analysis to quantify the uncertainty of intact rock strength. Journal of Rock Mechanics and Geotechnical Engineering 2018;10(1):11–31.
- Cook NGW. The failure of rock. International Journal of Rock Mechanics and Mining Sciences 1965;2(4):389–403.
- Day JJ, Hutchinson DJ, Diederichs MS. A critical look at geotechnical classification for rock strength estimation. In: Proceedings of the 46th US rock mechanics/geomechanics symposium. Chicago, USA: American Rock Mechanics Association (ARMA); 2012. paper 12-563.
- Deere DU. Geological considerations. In: Stagg KG, Zienkiewicz OC, editors. Rock mechanics in engineering practice. London: Wiley; 1968. p. 1–20.
- Endersbee LA, Hofto EO. Civil engineering design and studies in rock mechanics for Poatina underground power, Tasmania. Journal of the Institution of Engineers 1963;35:187–206.
- Fairhurst C. On the validity of the "Brazilian" test for brittle materials. International Journal of Rock Mechanics and Mining Sciences 1964;1(4):535–46.
- Flores G, Catalan A. A transition from a large open pit to a novel "macroblock variant" block caving geometry at Chuquibambilla Mine, Codelco Chile. Journal of Rock Mechanics and Geotechnical Engineering 2019;11(3) (in this issue).

- Franklin JA, Hoek E. Developments in triaxial testing technique. *Rock Mechanics* 1970;2(2):223–8.
- Gerogiannopoulos NG, Brown ET. The critical state concept applied to rock. *International Journal of Rock Mechanics and Mining Sciences and Geomechanics Abstracts* 1978;15(1):1–10.
- Griffith AA. The phenomena of rupture and flow in solids. *Philosophical Transactions of the Royal Society of London (Series A)* 1921;221(2):163–98.
- Griffith AA. Theory of rupture. In: *Proceedings of the 1st international congress on applied mechanics*. Delft, The Netherlands; 1924. p. 55–63.
- Hoek E. Fracture of anisotropic rock. *Journal of the South African Institute of Mining and Metallurgy* 1964;64(10):501–18.
- Hoek E. Rock fracture under static stress conditions. CSIR report MEG. 1965. p. 383. Pretoria, South Africa.
- Hoek E, Brown ET. *Underground excavations in rock*. London: Institution of Mining and Metallurgy; 1980a.
- Hoek E, Brown ET. Empirical strength criterion for rock masses. *Journal of the Geotechnical Engineering Division* 1980b;106(GT9):1013–35.
- Hoek E. Strength of jointed rock masses. *Géotechnique* 1983;33(3):187–223.
- Hoek E. Strength of rock and rock masses. *ISRM News Journal* 1994;2(2):4–16.
- Hoek E, Kaiser PK, Bawden WF. Support of underground excavations in hard rock. Rotterdam: A.A. Balkema; 1995.
- Hoek E, Brown ET. Practical estimates of rock mass strength. *International Journal of Rock Mechanics and Mining Sciences and Geomechanics Abstracts* 1997;34(8):1165–86.
- Hoek E, Marinov P, Benissi M. Applicability of the Geological Strength Index (GSI) classification for very weak and sheared rock masses. The case of the Athens schist formation. *Bulletin of Engineering Geology and the Environment* 1998;57(2):151–60.
- Hoek E, Marinov PG. Predicting tunnel squeezing problems in weak heterogeneous rock masses. *Tunnels and Tunnelling International* 2000;132(11):45–51.
- Hoek E, Carranza-Torres C, Corkum B. Hoek-Brown criterion – 2002 edition. In: Hammah R, Bawden W, Curran J, Telesnicki M, editors. *Mining and tunnelling innovation and opportunity, proceedings of the 5th North American rock mechanics symposium and 17th tunnelling association of Canada conference*. Toronto, Canada. Toronto: University of Toronto; 2002. p. 267–73.
- Hoek E, Marinov P, Marinov V. Characterization and engineering properties of tectonically undisturbed but lithologically varied sedimentary rock masses. *International Journal of Rock Mechanics and Mining Sciences* 2005;42(2):277–85.
- Hoek E, Diederichs MS. Empirical estimation of rock mass modulus. *International Journal of Rock Mechanics and Mining Sciences* 2006;43(2):203–15.
- Hoek E, Martin CD. Fracture initiation and propagation in intact rock – a review. *Journal of Rock Mechanics and Geotechnical Engineering* 2014;6(4):278–300.
- Jaeger JC, Cook NGW. *Fundamentals of rock mechanics*. 3rd ed. London: Chapman and Hall; 1969.
- Kaiser PK, Amann F, Bewick RP. Overcoming challenges of rock mass characterisation for underground construction in deep mines. In: *Proceedings of the 13th international congress on rock mechanics: ISRM congress 2015 – advances in applied & theoretical rock mechanics*. Montréal, Canada: International Society for Rock Mechanics; 2015. Paper 241.
- Kaiser PK, Kim B, Bewick RP, Valley B. Rock mass strength at depth and implications for pillar design. In: Van Sint Jan M, Potvin Y, editors. *Deep mining 2010, proceedings of the fifth international seminar on deep and high stress mining*, Santiago, Chile, Perth, Australia: Australian Centre for Geomechanics; 2010. p. 463–76.
- Kalamaris GS, Bieniawski ZT. A rock mass strength concept for coal incorporating the effect of time. In: Fuji T, editor. *Proceedings of the 8th congress on rock mechanics, ISRM*. Tokyo, Japan. Rotterdam: A.A. Balkema; 1995. p. 295–302.
- Kellaway M, Taylor D, Keyter GJ. The use of geotechnical instrumentation to monitor ground displacement during excavation of the Ingula power cavern, for model verification and design verification purposes. In: *Proceedings of South African tunnelling 2012 – lessons learned on major projects*, Ladysmith, South Africa. Johannesburg: Southern African Institute of Mining and Metallurgy; 2010. p. 1–23.
- Keyter GJ, Ridgeway M, Varley PM. Rock engineering aspects of the Ingula powerhouse caverns. In: *Proceedings of the 6th international symposium on ground support in mining and civil engineering construction*, Cape Town, South Africa. Johannesburg. Southern African Institute of Mining and Metallurgy; 2008. p. 409–45.
- Kovari K, Tisa A. Multiple failure state and strain controlled triaxial tests. *Rock Mechanics* 1974;7(1):17–33.
- Kruschke JK. *Doing Bayesian data analysis: a tutorial with R, JAGS and Stan*. 2nd ed. Amsterdam, New York: Academic Press; 2015.
- Langford JC, Diederichs MS. Quantifying uncertainty in Hoek-Brown intact strength envelopes. *International Journal of Rock Mechanics and Mining Sciences* 2015;74:91–104.
- Lau JSO, Gorski B. Uniaxial and triaxial compression tests on URL rock samples from boreholes 207-045-GC3 and 209-069-PH3. Divisional Report (Mining Research Laboratories (Canada)), MRL 92-025(TR). Ottawa: Mining Research Laboratories; 1992.
- Marinos P, Hoek E. GSI – a geologically friendly tool for rock mass strength. In: *Proceedings GeoEng 2000, International conference on geotechnical and geological engineering*. Melbourne, Australia, Lancaster, PA: Technomic Publishing Co.; 2000. p. 1422–40.
- Marinos P, Hoek E. Estimating the geotechnical properties of heterogeneous rock masses such as flysch. *Bulletin of Engineering Geology and the Environment* 2001;60(2):85–92.
- Marinos V, Marinov P, Hoek E. The geological strength index: applications and limitations. *Bulletin of Engineering Geology and the Environment* 2005;64(1):55–65.
- Marinos V. A revised geotechnical classification GSI system for tectonically disturbed rock masses, such as flysch. *Bulletin of Engineering Geology and the Environment* 2017;19:1–14. <https://doi.org/10.1007/s10064-017-1151-z>.
- Marinos V, Carter TG. Maintaining geological reality in application of GSI for design of engineering structures in rock. *Journal of Engineering Geology* 2018;239:282–97.
- McClintock FA, Walsh JB. Friction on Griffith cracks in rocks under pressure. In: *Proceedings of the 4th US National congress of applied mechanics*. Berkeley, USA. New York: American Society of Mechanical Engineers; 1962. p. 1015–21.
- Mogi K. Pressure dependence of rock strength and transition from brittle fracture to ductile flow. *Bulletin Earthquake Research Institute* 1966;44:215–32.
- Murrell SAF. The strength of coal under triaxial compression. In: Walton WH, editor. *Mechanical properties of non-metallic brittle materials*. London: Butterworths Scientific Publications; 1958. p. 123–45.
- Olavarria S, Adriasola P, Karzulovic A. Transition from open pit to underground mining at Chuquicamata, Antofagasta, Chile. In: *Proceedings of the international symposium on stability of rock slopes in open pit mining and civil engineering*. Cape Town: South Africa. Johannesburg: Institute of Mining and Metallurgy; 2006. p. 421–34.
- Perras MA, Diederichs MS. A review of the tensile strength of rock: concepts and testing. *Geotechnical and Geological Engineering* 2014;32(2):525–46.
- Ramamurthy T. Strength, modulus responses of anisotropic rocks. In: Hudson JA, editor. *Compressive rock engineering*, vol. 1. Oxford: Pergamon; 1993. p. 313–29.
- Ramsey JM, Chester FM. Hybrid fracture and the transition from extension fracture to shear fracture. *Nature* 2004;428:63–6.
- Read SAL, Richards LR, Perrin ND. Applicability of the Hoek-Brown failure criterion to New Zealand greywacke rocks. In: Vouille G, Berest P, editors. *Proceedings of the 9th international congress on rock mechanics*. Paris, France. Lisse: A.A. Balkema; 1999. p. 655–60.
- Ros M, Eichinger A. Experimental study of theories of rupture. *Non-metallic materials*, No. 28. Eidgenöss. Materialprüfungsanstalt, E.T.H Zurich; 1928 (in German).
- Rosengren KJ, Jaeger JC. The mechanical properties of an interlocked low-porosity aggregate. *Géotechnique* 1968;18(3):317–26.
- Rose ND, Scholz M, Burden J, King M, Maggs C, Havaei M. Quantifying transitional rock mass disturbance in open pit slopes related to mining excavation. In: *Slope stability 2018 – XIV International congress on energy and mineral Resources*. Seville, Spain: Asociación Nacional de Ingenieros de Minas; 2018. p. 1273–88.
- Sakurai S. *Back analysis in rock engineering*. ISRM Book Series, London: Taylor & Francis Group; 2017.
- Schwartz AE. Failure of rock in the triaxial shear test. In: *Proceedings of the 6th rock mechanics symposium*. Rolla, USA: University of Missouri; 1964. p. 109–51.
- Serafim JL, Pereira JP. Consideration of the geomechanical classification of Bieniawski. In: *Proceedings of the international symposium on engineering geology and underground construction*. Lisbon, Portugal. Lisbon: SPG/LNEC; 1983. p. 33–44.
- Sheorey PR. *Empirical rock failure criteria*. Rotterdam: A.A. Balkema; 1997.
- Stephens RE, Banks DC. Moduli for deformation studies of the foundation and abutments of the Portuguese Dam - Puerto Rico. In: Khair AW, editor. *Rock mechanics as a guide for efficient utilization of Natural resources, proceedings of the 30th US symposium on rock mechanics*. Morgantown, USA. Rotterdam: A.A. Balkema; 1989. p. 31–8.
- Ulusay R, Hudson JA, editors. *The complete ISRM suggested methods for rock characterization, testing and monitoring: 1974–2006*. Ankara: ISRM Turkish National Group; 2007.
- Vlachopoulos N, Diederichs MS, Marinov V, Marinov P. Tunnel behaviour associated with the weak Alpine rock masses of the Driskos Twin Tunnel system, Egnatia Odos Highway. *Canadian Geotechnical Journal* 2012;50(1):91–120.
- Von Kármán T. Festigkeitsversuche unter allseitigem Druck. *Zeitschrift Verein Deutscher Ingenieure* 1911;55:1749–57 (in German).
- Walton S, Hasan O, Morgan K, Brown MR. Modified cuckoo search: a new gradient free optimization algorithm. *Chaos, Solutions and Fractals* 2011;44(9):710–8.
- Zuo JP, Li HT, Xie HP, Ju Y, Peng SP. A nonlinear strength criterion for rocklike materials based on fracture mechanics. *International Journal of Rock Mechanics and Mining Sciences* 2008;45(4):594–9.
- Zuo JP, Liu H, Li H. A theoretical derivation of the Hoek-Brown failure criterion for rock materials. *Journal of Rock Mechanics and Geotechnical Engineering* 2015;7(4):361–6.



**Dr. Evert Hoek** was born in Zimbabwe, graduated in mechanical engineering from the University of Cape Town and became involved in the young science of rock mechanics in 1958 when he started working in research on the problems of brittle fracture of rock, associated with rockbursts in very deep mines in South Africa. His degrees include a PhD from the University of Cape Town, and a DSc (Engineering) from the University of London. He spent 9 years as a Reader and then Professor of Rock Mechanics at the Imperial College of Science and Technology in London, 12 years as a Principal of Golder Associates in Vancouver, Canada, 6 years as an Industrial Research Professor of Rock Engineering at the University of Toronto, Canada, and 25 years as an independent consulting engineer, living in Vancouver. His consulting work involved

major mining and civil engineering projects including rock slopes, dam and bridge foundations and underground caverns and tunnels. He retired from active consulting in 2013 to the age of 80, but he maintains an interest in education in rock engineering.